46. ORGANIC-MATTER-RICH AND HYPERSILICEOUS APTIAN SEDIMENTS FROM WESTERN MID-PACIFIC MOUNTAINS, DEEP SEA DRILLING PROJECT LEG 62[1]

Frédéric Mélières, Laboratoire de Géologie Dynamique, Université Pierre et Marie Curie, 75230 Paris Cedex 05, France
and
Gérard Deroo and Jean-Paul Herbin, Institut Français du Pétrole, 4 Avenue de Bois-Préau, 92502 Rueil-Malmaison, France

ABSTRACT

A 15-meter sequence of early Aptian organic-matter-rich sediments, cored at Deep Sea Drilling Project Site 463 (western Mid-Pacific Mountains) has been submitted for detailed mineralogical studies (XRD, SEM) and organic-carbon characterization. Although intense diagenesis has obscured the sedimentary record of depositional conditions, the history has been tentatively reconstructed. Through sustained volcanic activity and alteration processes on the archipelago, large amounts of silica were released into the sea water, resulting in a "bloom" of radiolarians. Hard parts settled in large amounts, yielding a hypersiliceous sediment; amorphous silica was diagenetically transformed into chalcedony, opal-CT and clinoptilolite through dissolution and recrystallization. Oxidization of part of the radiolarian soft parts (1) depleted the sea water in dissolved oxygen, allowing the burial of organic matter, and (2) generated carbon dioxide which led to dissolution of most of the calcareous tests. Moderate depositional depth and a high sedimentation rate are though to have prevailed during this episode. An immature stage of evolution is assigned to the studied organic matter, which is of two origins: autochthonous marine material, and allochthonous humic compounds and plant debris. Rhythmic sedimentation characterizes the distribution of the organic matter; each sequence shows (1) an upward progressive increase in organic-carbon content, and (2) an upward enrichment in marine organic matter.

INTRODUCTION

This report is an extended account of the mineralogy and organic geochemistry of early Aptian sediments cored at DSDP Site 463 (Fig. 1), in the western Mid-Pacific Mountains (central subtropical North Pacific). These sediments, very succcessfully recovered in a complete sequence in Cores 70 and 71 (Fig. 2) are characterized by a high organic-carbon content and the frequent occurrence of volcanogenic constituents. The sediments are cyclic alternations of silicified limestone, ashy limestone, and carbonaceous limestone; colors are generally dark, ranging from greenish gray (silicified limestone) to olive-black (ashy and carbonaceous limestone); all this material is fine-grained and frequently laminated in the darker lithologies, whereas the lighter ones show discrete burrowing (see Site 463 report, this volume).

The occurrence of organic carbon and volcanogenic constituents together led to detailed investigations of the mineralogy of the sediments and the nature, origin, and history of the organic fraction. For these purposes, 150 samples were selected in Cores 70 and 71 (a 15-meter sequence). To try to understand the dark facies within the frame of general sedimentation in Aptian time at Site 463, 50 additional samples were taken in Cores 69 and 72.

[1] *Initial Reports of the Deep Sea Drilling Project*, Volume 62.

MINERALOGY

Analytical Methods

Qualitative and quantitative mineralogical analyses were carried out on the bulk sediment by X-ray diffractometry. The analytical procedure, basically operating on non-oriented powder with the use of an internal standard (NaF), is described in detail elsewhere (Mélières, 1974). A résumé of the basic steps is given in Mélières (1978).

The mineralogical data are graphically represented in Figure 3 (back pocket, this volume), and they are listed in Table 1. Comments on unusual crystallographic data are given in the text.

Feldspars

Feldspar minerals are represented almost throughout the studied section. They consist of both K-feldspar and plagioclase, but because of their very low concentration (absence to few percent), their exact nature cannot be precisely determined from the routine diffractometry data.

Plagioclase occurs only in Cores 70 and 71, where it shows a good correlation with, but remains subordinate to, K-feldspar.

Sample 463-72-2, 13–14 cm yielded a minor lithology consisting of a micro-bed of fine-grained, dark sand, in which the K-feldspar content reaches 18%. X-ray diffractometry revealed sanidine (K was confirmed through X-ray microprobe). SEM observation shows that the

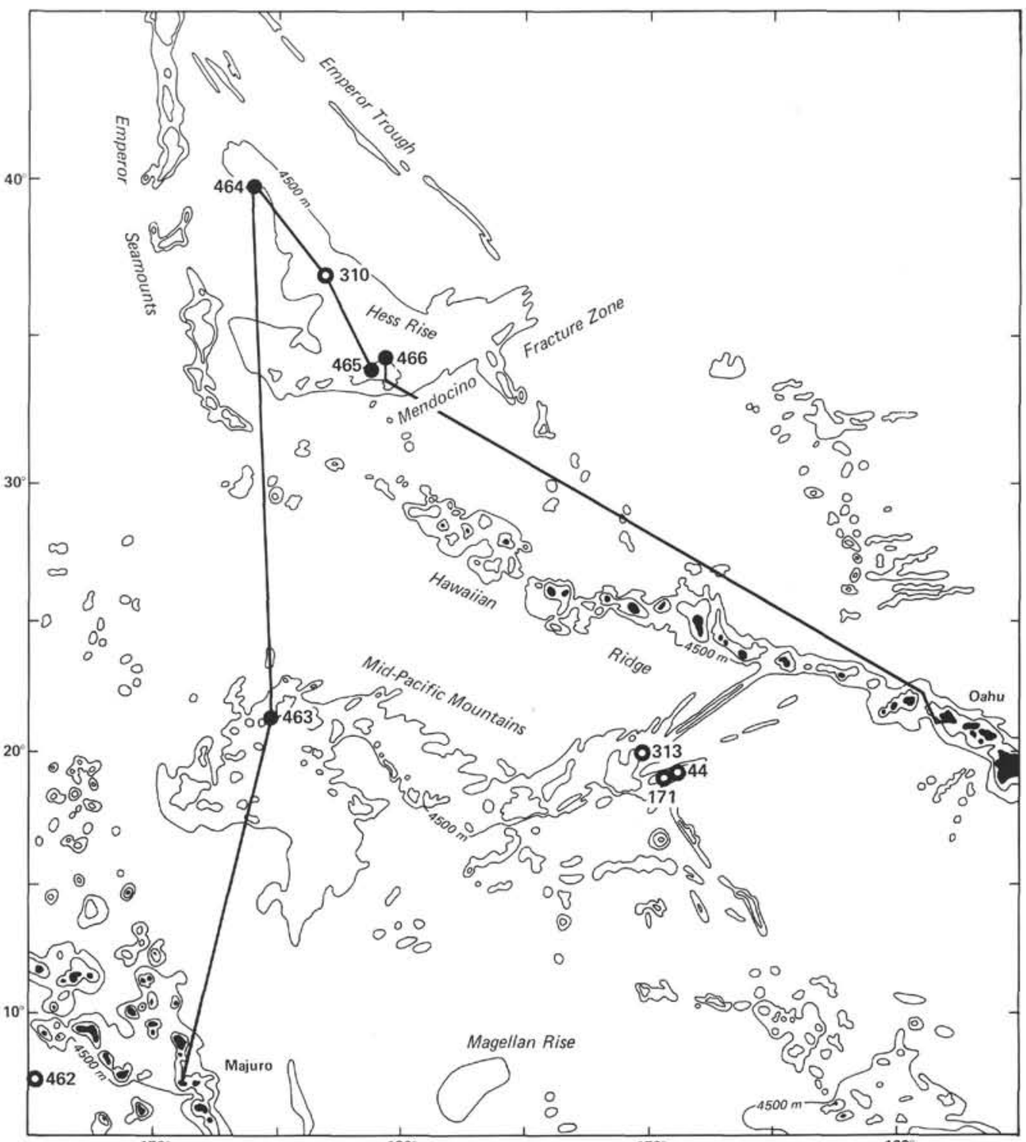

Figure 1. Location of Site 463, and other DSDP sites.

feldspar grains are well rounded, indicating that they are detrital.

These data suggest that the K-feldspar is terrigenous, probably from on-shore, evolved volcanic material. The alkalic nature of the feldspar suggests that this volcanic material did not originate from the early archipelagic framework, but more likely from a partly differentiated magma. This indicates that at least a part of the western Mid-Pacific Mountains already existed as emergent land masses in early Aptian time.

Clay Minerals

Clay minerals are represented here exclusively by 10-Å phyllosilicate structures, giving X-ray diffraction patterns characterized in the untreated sample by a diffuse "bump" between 10 Å and 17 Å, and in the glycolated sample by (1) a broad but well-centered 17-Å peak interpreted as smectite and (2) a broad but well centered 10-Å peak interpreted as illite.

These 10-Å phyllosilicate structures appear to be characterized by a complex interlayer population consisting of various cations (Ca, K, Na, etc.) yielding various hydration states, and consequently various basal spacing, ranging from 10 Å to 17 Å. Therefore, the term "illite" is not to be taken here in its general sense ("micaceous" clay), but more likely as indicating the K-interlayer, saturated, non-expandable fraction of the 10-Å phyllosilicate structures.

Smectite and illite occur throughout the studied section, except in the upper part of Core 69, where they are sporadic. They are present in rather moderate amounts, 1 to 2% for illite, and 5% (average) for smectite,

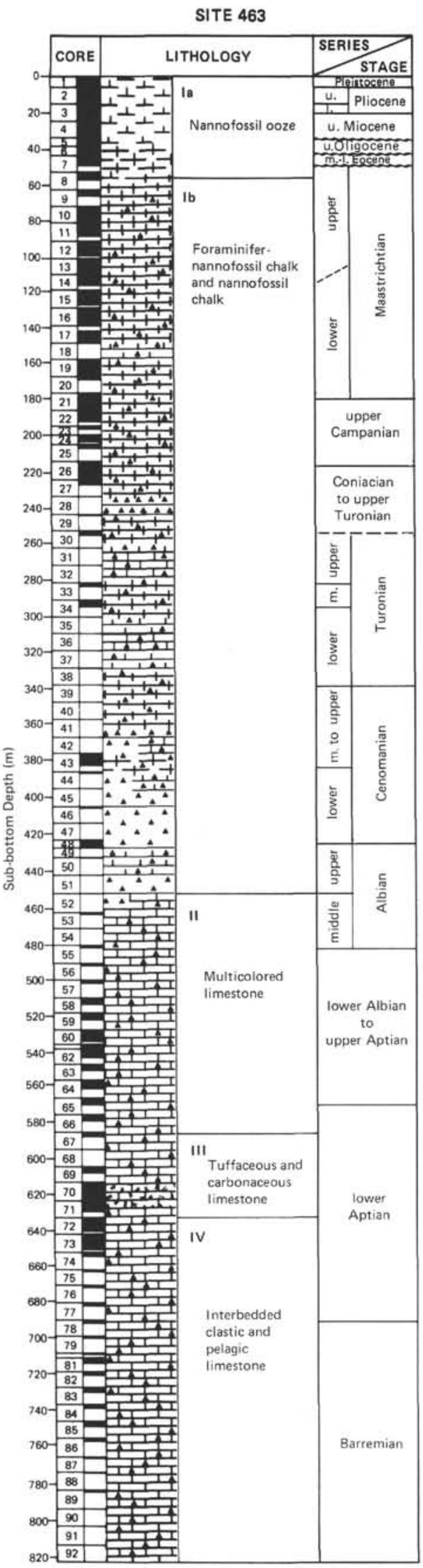

Figure 2. Lithologic column and biostratigraphic zonation of DSDP drill Site 463.

although the latter may occur in much higher values, reaching 50% of the sediment in the upper part of Section 1 of Core 71.

SEM and optical microscope observations reveal that smectite results from transformation of volcanogenic material (Plates 1 and 2). DTA analysis and systematic study of the (060) X-ray-diffraction peak show that the smectite belongs to the beidellite–nontronite series, displaying an octahedral iron content ranging from 35 to 60%. This seems to confirm the relation of the smectite with volcanogenic material.

Illite and smectite show good correlation in the variation of their concentrations, except for high smectite values. This suggests either that both minerals are originally closely related and derived from the same sources (except during the deposition of smectite-rich sediments), or that illite resulted from diagenetic transformation of part of the smectite during periods of sea water (or interstitial water close to sea water) contact long enough to allow potassium to be accommodated as an interlayer cation. The latter hypothesis seems more likely in the light of Core 69 data: within the lower half of Section 2 and in Section 3, the illite/smectite ratio is the highest of the entire studied sequence, and the minerals show an excellent correlation. This episode is immediately followed by normal marine, almost exclusively carbonate sedimentation, the deposition rate of which appears to have been much slower than that existing during the previous deposition of sediment.

Consequently, the best conditions for diagenetic evolution of smectite into illite seem to have been realized during that time, because of the possibility of long contact with interstitial waters close to sea water, which resulted from the high porosity of the overlying carbonate beds. Actually, the relationship between illite and smectite within Core 69 seems to indicate the (early?) diagenetic nature of illite in this case.

In the upper part of Core 69, and in Core 72, smectite shows good correlation with K-feldspar. This confirms the terrigenous nature of smectite, and implies that this mineral was generated on shore through alteration of volcanogenic material. (The formation of iron-bearing smectites through deuteric alteration of the base of terrestrial lava flows has been recently pointed out [Mélières and Person, 1978]). In Core 72, Section 2, the smectite peak, indicates an unquestionably terrigenous smectite: there is a significant amount of kaolinite, reaching 7% in a sandy micro-bed which could be interpreted as a distal turbidite.

In smectite-rich sediments of Cores 70 and 71, there is no correlation between smectite and K-feldspar. In such cases the smectite and volcanogenic material are thought to be primarily associated, and the abundance peaks of smectite are interpreted as direct echoes of volcanic events. Such events would have induced high sedimentation rates, preventing the deposited material from long and close contact with sea water. Consequently, the smectite would have been unable to partly convert to illite. This seems to have occurred, because there is no correlation between smectite and illite abundance peaks.

Table 1. Mineralogy of Cores 69 through 72, Site 463.

Sample	Feldspars				Clinop-	Quartz		Opal-CT		Calcite			Siderite						Amorphous
(interval in cm)	Plag.	K	Illite	Smectite	tilolite	%	Cryst.	%	B/A	%	Cryst.	$MgCO_3$ (%)	%	Chem.	Pyrite	Kaolinite	Barite	Halite	Material
463-69-1, 5-7			T	1.0		6.3	0.90			82	1.90	0.0						0.3	10
69-1, 61-63			T	1.7		2.0	0.90			83	1.20	0.0						0.4	12
69-1, 75-77			T	2.4		3.5	0.90			78	2.02	0.0						0.4	15
69-1, 89-91			T	1.2		2.2	0.90			86	2.05	0.0	1.6	Ca 6				?	9
69-1, 104-106				T		2.9	0.90			80	1.95	0.0						0.5	16
69-1, 107-109			T	0.9		1.7	0.90			87	2.25	0.0						0.3	10
69-1, 110-112		8.0		43						8.9	?	0.0	9.0	Ca 8				?	31
69-1, 114-116		3.3	2.9	16		1.9	0.90			33	1.55	0.0	6.8	Ca 8				?	36
69-1, 119-121						5.4	0.90			80	2.02	0.0						0.4	12
69-1, 131-132				T		3.4	0.90			80	1.48	0.0						0.3	15
69-1, 139-141				T		3.3	0.90			81	1.97	0.0						0.3	15
69-2, 17-19			T	0.8		5.3	0.90			81	1.55	0.0						0.4	12
69-2, 49-51				T		1.6	?			84	1.55	0.0						0.5	14
69-2, 82-84	0.3	0.3	2.2	2.0		28	0.80			55	1.55	0.0						0.4	11
69-2, 108-110			2.0	2.4		7.4	1.00			78	2.80	0.0						0.3	9
69-2, 122-123			1.2	2.7		24	0.90			38	2.80	0.7						T	34
69-2, 146-148			4.2	8.2		9.3	0.90			27	4.05	0.0	21	Ca 10				?	30
69-3, 14-15		1.2	2.5	3.1		23	0.95			52	2.75	0.5						0.2	18
69-3, 22-24		T	3.4	6.0	6.1	8.6	1.10	5.1	?	45	3.05	0.0						T	25
69-3, 31-32			1.5	2.2		6.3	1.05	33	0.46	37	3.10	0.0						T	20
69-3, 39-41			1.1	1.0		15	1.15	40	0.45	27	3.05	0.0					T	?	16
69-3, 46-48			1.7	1.6	1.8	2.9	1.00	39	0.47	37	2.95	0.0					T		16
70-1, 4-5		0.7	2.7	7.6	11	6.4	1.20	17	0.40	22	3.55	0.8	0.9	?	2.4		0.3	?	29
70-1, 7-8			0.8	0.7		9.0	1.10	13	0.42	41	3.05	0.0							35
70-1, 23-24		0.6	1.6	13	5.7	9.7	1.30	4.6	?	35	3.05	0.0	5.0	Ca 9			0.3		34
70-1, 27-29		T	1.2	3.8	1.2	6.4	1.30	30	0.40	41	5.10	0.0					T		16
70-1, 37-38	T	0.5	2.6	4.9		19	1.25	6.4	?	41	4.30	0.5							25
70-1, 41-43	T	0.4	0.2	1.5		24	1.10	33	0.44	23	4.55	0.0						T	17
70-1, 52-53	T	0.5	1.6	4.3	4.4	17	1.40	10	0.41	48	4.67	0.0	1.1	?				?	12
70-1, 67-68			0.9	3.4		18	1.40	15	0.41	45	4.80	0.5					T		17
70-1, 80-82			1.2	1.7		16	1.00	44	0.45	19	2.80	0.0						T	18
70-1, 89-91		T	1.7	7.4	6.3	34	1.10	28	?	9.1	3.05	0.0					0.9		12
70-1, 96-98	0.5	0.9	2.6	7.1	6.7	4.3	0.90	41	0.42	11	1.55	0.0			1.9		0.5		23
70-1, 101-102	T	0.3	1.0	2.9		13	0.85	39	0.45	21	2.30	0.0			0.8		0.5		21
70-1, 108-109	0.5	0.5	2.9	11	1.8	9.7	1.20	36	0.47	16	2.92	0.0			1.4				20
70-1, 117-118	T	0.7	1.1	17	40	13	1.20	11	0.43	3.9	?	?							13
70-1, 128-130		T	1.5	2.1		14	1.00	40	0.44	21	2.92	0.0						?	21
70-1, 138-139	T	0.8	0.6	11	15	8.4	1.25	4	?	31	3.55	0.5			1.0		0.4	?	27
70-1, 143-145		0.9	2.7	4.8		20	1.35	26	0.41	27	3.80	0.0			2.3			?	16
70-2, 4-5	0.4	0.8	1.5	3.2		9.6	1.30	37	0.41	30	4.55	0.7			6.6			T	11
70-2, 9-10	T	0.5	1.1	2.2		8.7	1.40	33	0.43	41	5.05	0.9			1.7		T		11
70-2, 27-29	T	0.9	1.2	5.7	2.4	18	1.30	8.6	?	37	4.42	0.7	3.1	Ca 9	2.9		0.4	?	19
70-2, 34-35			0.7	1.4		30	1.15	35	0.44	17	4.55	0.7							15
70-2, 46-47		0.6	0.7	2.4		10	1.20	31	0.41	44	6.05	0.7			1.9			?	9
70-2, 53-54		0.3	1.0	3.0		11	0.95	44	0.44	19	3.05	0.0			0.6		0.2	?	20
70-2, 68-70		T	0.7	2.2		13	0.90	51	0.44	4.6	?	?			1.5				26
70-2, 77-78		T	1.2	2.8	0.9	18	1.10	33	0.42	18	7.05	0.8			3.2				22
70-2, 85-86		T	1.3	3.0		18	0.90	52	0.43						2.6				23
70-2, 91-94	0.5	0.8	2.0	4.6		10	1.00	53	0.44	1.5	?	?			3.9				23
70-2, 97-99	0.4	0.8	2.9	8.2		20	1.20	17	?	15	5.05	0.6			2.0				33
70-2, 101-103	T	0.6	1.9	5.0		11	1.20	35	0.43	21	7.80	0.5			1.3		1.1	?	23
70-2, 109-111			1.2	1.9		29	0.90	44	0.45	2.7	?	?							21
70-2, 121-122	T	0.4	2.1	5.9	0.4	17	1.30	14	0.44	20	4.80	0.5			2.2		0.6		37
70-2, 127-129	0.5	0.8	2.9	5.2	T	19	1.30	14	?	27	5.05	0.9			1.7		0.4	?	28
70-2, 137-139			2.4	2.5		24	1.00	48	0.49	13	3.30	0.0					0.5		19
70-2, 144-146	0.6	0.3	2.9	4.0		8.8	1.00	54	0.51	14	4.80	0.6					0.5		14
70-3, 2-3	0.4	0.3	1.1	2.7		5.3	1.20	44	0.47	30	4.35	0.9			1.2		0.4	T	14
70-3, 16-17			1.0	1.5		24	0.90	36	0.49	20	4.55	0.8					0.4		17
70-3, 19-20			1.0	1.5		22	0.90	48	0.48	5.4	2.80	0.6					0.3		21
70-3, 20-21			0.7	1.2		16	1.00	43	0.49	12	3.55	0.6			2.6		0.5	T	24
70-3, 25-27	0.8	0.8	1.4	4.8	1.8	6.4	0.70	54	0.42	3.2	?	0.0			9.0		0.7		17
70-3, 30-31	0.4	0.4	1.4	3.4	1.8	5.7	0.90	47	0.43	4.0	?	0.0			4.4		0.5		31
70-3, 31-32	0.4	0.5	1.3	3.2	2.9	8.6	1.05	27	0.44	21	5.37	0.5			6.5		1.1		27
70-3, 39-40	0.4	0.4	1.2	8.3	11	7.7	0.90	36	0.42	0.7	?	?			2.2		T		32
70-3, 43-44		T	0.7	1.3		25	1.10	50	0.46	1.2	1.30	0.0			1.1		T		20
70-3, 47-49			T	1.0		23	1.00	55	0.45						0.8				20
70-3, 55-56			0.8	2.0		17	0.95	52	0.45	2.1	?	?			2.0		T		24
70-3, 64-65			1.1	3.2		6.2	0.80	56	0.46	13	4.05	0.6			1.2		T		19
70-3, 75-77			0.8	2.9		8.4	0.80	63	0.46	1.8	?	?			1.4		0.3		21
70-3, 81-82			1.0	5.6	2.2	7.2	0.80	53	0.42	0.4	?	?			2.1		0.4		28
70-3, 89-90	T	T	1.3	1.6		26	0.80	47	0.46	0.8	?	?			0.8		0.3		22
70-3, 103-104	T	0.5	0.7	3.3	1.5	7.2	0.80	54	0.42	6.8	?	0.4			3.0		T		22
70-3, 117-119	T	0.5	1.4	7.7	10	4.5	0.65	45	0.42	5.2	3.55	0.4			2.3		0.4		23
70-3, 127-129	0.6	0.6	0.7	2.7	0.4	8.9	0.90	55	0.43	6.4	?	0.5			T				24
70-3, 134-136	0.5	0.6	0.6	2.4		6.3	0.70	67	0.45	3.0	?	?			T				19
70-3, 140-142			0.8	1.0		23	0.80	50	0.47	6.7	4.30	0.6			0.9				17
70-3, 142-144	0.5	0.6	2.3	12	12	9.5	0.90	23	0.43	6.6	?	0.5			1.4		T		31
70-4, 5-7			0.3	5.4	0.5	5.9	0.90	52	0.46	5.6	?	0.6							30
70-4, 18-20		1.0	0.8	10	28	9.0	1.10	12	?	24	5.55	1.4			?		0.6		16
70-4, 31-32	T	T	0.6	9.5	11	3.3	0.80	44	0.42	3.9	?	0.6			1.0		0.4		25
70-4, 42-43	0.4	0.4	1.3	12	6.6	4.5	0.90	48	0.42	2.6	?	0.6			0.8				23
70-4, 56-57	0.2	0.4	1.4	18	10	6.5	1.10	10	?	35	8.17	1.0			?		0.5		18
70-4, 63-64			0.7	2.1	0.9	4.6	0.90	48	0.43	36	8.68	1.5			?				7
70-4, 78-79			0.8	2.1		20	0.95	50	0.45	8.7	5.70	1.4			4.2				14
70-4, 84-85	T	0.5	1.9	7.7	1.3	16	1.10	35	0.40	5.2	5.30	1.4			4.0				28
70-4, 96-97	T	0.6	1.2	6.4	0.8	11	1.10	42	0.44	7.8	7.55	2.0			2.8		T		27
70-4, 104-105				2.6		18	0.95	63	0.46	0.8	?	?			1.2		T		14
70-4, 111-113	T	1.0	2.0	8.1	2.3	5.4	0.80	43	0.41	6.1	3.80	0.6			4.1				28
70-4, 124-125	0.5	0.5	1.2	5.7	0.7	7.5	1.00	58	0.43	1.5	?	?			2.6				21
70-4, 133-135	0.3	0.5	1.2	6.9	0.4	14	1.05	35	0.42	6.2	5.55	1.2			2.2		0.3		33
70-4, 144-145			1.3	5.2		14	1.15	51	0.46						1.5				27
70-5, 0-1	T	T	0.6	23	18	8.8	1.00	5.4	?	6.5	4.30	1.2			9.6		0.6		27
70-5, 16-17			0.6	0.7		24	0.85	50	0.45	1.3	?	?			2.5		0.5		20
70-5, 27-28	0.7	0.8	2.2	9.5	0.3	17	1.15	9.6	?	5.5	?	?	2.1	Ca 10	3.6		0.4		48
70-5, 37-38	T	0.5	1.1	0.8		7.6	0.90	76	0.47	1.0	?	?			1.7				11
70-5, 47-48	T	T	1.5	2.4	T	4.2	1.00	71	0.48	7.2	7.30	2.0			3.2		T		10
70-5, 53-54	0.6	0.7	1.2	6.1	1.9	5.9	0.90	44	0.47	17	6.17	1.6			2.1		0.5		20

Table 1. (Continued).

Sample (interval in cm)	Feldspars Plag.	Feldspars K	Illite	Smectite	Clinop-tilolite	Quartz %	Quartz Cryst.	Opal-CT %	Opal-CT B/A	Calcite %	Calcite Cryst.	Calcite $MgCO_3$ (%)	Siderite %	Siderite Chem.	Pyrite	Kaolinite	Barite	Halite	Amorphous Material
70-5, 60-61	2.6	3.1	2.2	11	5.0	16	1.10	2.8	?	18	6.05	0.7			2.9		0.7		30
70-5, 72-73	T	T	1.0	1.9		18	0.90	39	0.44	27	7.30	1.2			T				13
70-5, 84-85		0.9	1.1	14	18	7.7	0.90	3.8	?	38	7.42	2.0			3.0		0.4		13
70-5, 100-101						27	0.95	27	?	9.7	4.80	1.2			22				14
70-5, 105-108		T	0.5	0.9		22	0.90	27	0.46	27	4.55	1.0			1.1		0.4		11
70-5, 129-130	0.6		1.5	1.3		18	0.85	41	0.44	25	5.05	1.6			1.8				10
70-5, 146-147	0.3	0.5	1.8	4.7	0.4	18	1.05	32	0.40	25	5.05	2.2			2.3		0.4		14
70-6, 4-5	T	0.5	2.7	2.7		22	0.85	39	0.42	3.6	?	?			2.9		0.3	0.3	26
70-6, 13-14	0.4	0.6	1.6	3.6		27	1.15	21	0.40	24	3.55	1.4			2.7				19
70-6, 23-24	T	0.6	1.0	2.5		28	1.20	23	0.41	30	3.55	1.0			2.1		0.3		12
70-6, 35-36			1.0	1.3		32	1.00	32	0.46	4.9	3.30	?			11		T		27
70-6, 45-46	0.3	0.3	2.2	2.5		26	0.80	42	0.44	3.4	3.30	?			10		1.2	?	22
70-6, 60-61	0.3	0.5	2.1	3.9		24	0.80	36	0.45	9.1	6.30	1.0			2.2		0.5	0.3	21
70-6, 75-76	T	T	2.2	2.7		23	0.85	36	0.45	13	6.55	0.7			1.9		0.6	0.3	20
70-6, 85-86	0.9	1.2	2.8	7.0	1.2	16	1.00	32	0.43	17	6.80	0.6			1.8		0.5	0.2	19
70-6, 95-96	0.6	0.6	1.4	2.3		15	0.85	54	0.47	3.0	4.30	?			1.6		0.4	?	21
70-6, 105-106	1.2	1.4	3.2	5.6		15	0.95	43	0.46	6.3	5.55	1.0			2.1		0.4	?	21
70-6, 122-123			1.0	1.6		30	0.95	47	0.45	1.1	?	?			1.0				18
70-6, 134-135	1.1	1.3	2.9	5.3	7.8	17	1.10	22	0.43	3.0	?	?			14		0.5		25
70-6, 144-145	0.6	0.8	1.2	2.2	0.8	9	0.90	63	0.48	0.6	?	?					T		21
70-7, 2-3	0.9	0.8	1.5	4.4		13	0.95	53	0.43	0.4	?	?					0.4		25
70-7, 10-11	1.1	0.6	0.7	14	25	3.7	0.80	32	0.38	T	?	?					0.7		22
70-7, 29-30	0.7	0.4	0.7	21	30	6.8	1.10	20	0.39	14	7.05	3.1	2.9	Ca 10			0.4		13
70,CC, 8-9	0.5	0.5	0.6	17	31	9.4	1.00	16	0.36	11	6.67	2.9	3.8	Ca 10			0.7		9
70,CC, 18-19	0.6	0.8	0.6	13	25	7.4	1.00	28	0.35								0.4		24
71-1, 2-3	?		2.2	40	19	2.0	0.70			26	6.80	3.0	5.8	Ca 8					4
71-1, 17-19	?		1.6	13	15	2.5	0.65	41	0.41										26
71-1, 32-33	?			50	16	1.8	0.60	6	?	8.5	?	2.5	1.5	Ca 4					16
71-1, 38-39	?		1.9	4.5	3.6	8.7	0.80	56	0.44	1.5	?	1.8							23
71-1, 56-58			1.5	2.4		29	0.85	44	0.46	0.8	?	?							22
71-1, 69-71	T	T	1.8	3.1		30	1.00	48	0.47								0.4		16
71-1, 83-84		3.1	1.3	3.1		27	1.20	4.8	?	1.9	?	4.0	3.0	Ca 7			0.7		49
71-1, 87-89	1.3	1.5	3.9	13		28	1.20	12	?	1.5	?	4.5	1.0	Ca 7					37
71-1, 98-99	0.8	1.0	1.1	4.6	0.5	20	1.00	39	0.43										33
71-1, 107-112	0.3	0.5	1.0	1.4		32	1.00	33	0.45									T	32
71-1, 117-118	0.8	0.6	0.7	2.8		17	0.95	43	0.42									T	35
71-1, 123-124	0.9	1.2	4.0	2.3		19	0.80						0.7	Ca 7				?	51
71-1, 127-128			1.5	2.5		21	1.25	7.8	?	45	5.30	1.3						0.2	22
71-1, 138-139			T	T		13	1.35	46	0.36	46	4.30	1.3						0.2	5
71-1, 144-145			T	T		34	1.05	35	0.38	25	4.30	1.3						0.2	5
71-2, 2-3			1.1	1.7		17	1.00	31	0.41	19	3.30	1.0					0.4	0.2	29
71-2, 14-15		1.3	1.1	9.8		15	1.10			30	3.55	1.0					T	?	42
71-2, 23-25	0.4	0.4	2.0	3.1		11	1.10	25	0.45	27	3.42	1.0							31
71-2, 31-32	T	T	1.3	1.9		7.6	1.20	39	0.42	35	5.80	2.3						T	15
71-2, 38-39	T	T	1.0	1.7		7.7	1.20	50	0.41	21	8.05	1.6						0.4	18
71-2, 58-59	1.2	1.8	2.1	13		20	0.90	4.1	?	9.9	3.80	1.3	3.6	Ca 6			0.6		43
71-2, 62-63	0.5	0.8	2.3	9.2		19	1.05	6.0	?	33	6.17	1.3							29
71-2, 96-97	0.5	1.2	2.1	6.3		21	1.05	3.3	?	41	3.80	1.0					T	T	24
71-2, 114-115		0.4	0.9	2.7		19	1.20	2.2	?	47	4.30	1.3						T	27
71-2, 132-134			0.5	1.7		28	1.10	2.8	?	42	4.20	1.2						T	25
71-2, 142-144			1.0	1.8		29	1.20	4.0	?	52	4.70	1.3						T	13
71-3, 4-5			1.1	1.6		21	1.10	2.0	?	57	3.05	0.9							17
71-3, 13-14		0.6	2.4	4.8		22	1.30			48	4.05	1.0							22
71-3, 27-29		0.5	1.9	4.2		13	1.10	12	?	45	2.80	0.0							23
71-3, 39-40		0.5	2.0	3.7		9.3	1.20	9	0.33	47	2.55	0.0					T		28
71-3, 52-57		1.6	2.0	13		12	1.25			39	2.55	0.0	1.0	Ca 6			T		31
71-3, 73-74		0.5	0.7	4.1	1.3	6.2	1.40	13	0.38	56	2.30	0.0						?	19
71-3, 95-97			0.9	0.8		25	1.00	25	0.39	21	3.05	0.3						T	27
71-3, 110-112				2.0		25	1.25	8.4	?	55	2.80	0.0						T	9
71-3, 123-125						20	1.10	11	?	60	2.30	0.0						0.4	8
71-3, 145-146						32	1.10	14	0.36	30	3.05	0.4						0.3	23
71-4, 13-14			0.7	1.8		17	1.00			67	3.17	0.4						0.2	14
71-4, 19-20			0.6	1.4		12	1.00			62	2.62	0.0						0.2	23
71-4, 65-67				1.4		10	1.20			62	2.55	0.0						T	26
71-4, 72-73				1.8		13	1.00			67	2.20	0.0					T	T	18
71-4, 75-76	0.6	1.7	4.9	7.8		10	1.10			45	2.80	0.0					0.5		29
71-4, 76-77		T	0.3	1.0		7.0	1.10			85	1.92	0.0					T	0.3	6
71-4, 87-89			2.0	3.5		8.8	1.00			74	2.55	0.0					T	0.3	12
71-4, 92-93		0.7	2.8	6.9		15	1.00			54	2.92	0.0					0.3	0.3	19
71-4, 93-94				1.7		7.5	1.20			79	2.80	0.0					T	?	11
72-1, 4-6			2.5	3.7		12	1.05			77	4.30	0.5							4
72-1, 13-15			2.3	5.5		22	1.30	1.0	?	51	3.18	0.3							
72-1, 18-19			1.9	3.6		15	1.10	2.0	?	60	3.25	0.5							17
72-1, 22-23			1.3	1.8		25	0.90	2.7	?	61	3.22	0.3						T	8
72-1, 42-44		0.6	0.9	2.4		19	1.10	15	?	48	3.15	0.7		*18*			1.0	0.6	12
72-1, 58-59			1.1	2.5		19	1.30	3.4	?	51	3.05	0.3	T						22
72-1, 63-64		1.2	1.5	7.6		19	1.30	2.1	?	44	3.10	0.4							24
72-1, 71-73		0.5	2.3	3.3		12	1.10	18	0.41	43	2.62	0.7						0.2	20
72-1, 81-82		0.6	1.6	2.3		25	1.00	26	0.41	24	2.80	0.2						0.6	19
72-1, 93-94		0.3	1.3	2.3		10	1.00	19	0.42	54	2.05	0.0					?	0.8	12
72-1, 99-101		0.5	1.6	2.3		15	1.20	3.7	?	55	3.30	0.3							21
72-1, 116-118		0.4	1.4	2.2		17	1.40	14	0.41	55	2.55	0.0	1.5	Ca 6					8
72-1, 134-135		T	0.7	3.2		11	1.40	8.8	?	61	2.10	0.0						T	15
72-2, 9-11		0.6	1.3	5.0		9.3	1.30	3.6	?	61	1.30	0.0	0.6	Ca 4				T	24
72-2, 13-14		2.8	0.6	19						37	1.30	0.0	0.6	Ca 4		0.4			39
72-2, 19-20		0.4	0.7	2.6		4.9	1.30	20	?	60	2.42	0.2					T	0.4	10
72-2, 32-34		0.3	0.3	1.5		6.2	1.40	20	0.41	47	2.30	0.0						0.3	24
72-2, 48-49		0.8	0.8	3.2		11	1.30	15	?	49	2.62	0.1	T					T	19
72-2, 52-53		0.8	1.6	4.8		16	1.30	5.0	?	50	2.67	0.0	?						21
72-2, 55-56		0.5	1.0	3.2		16	1.30	5.3	?	48	2.30	0.0	?						26
72-2, 66-68			1.7	1.6		21	1.10	29	0.39	29	3.80	0.3						0.2	17
72-2, 77-78	?	0.7	2.7	3.1		7.6	1.20	21	?	41	3.75	0.3					0.2		23
72-2, 83-84	?	0.7	1.0	6.6		11	1.20	5.2	?	46	2.55	0.1	?				T	T	28
72-2, 90-91		0.2	0.8	1.1		9.0	1.20	27	0.42	42	1.80	0.0						0.2	19
72-2, 102-104		0.5	1.6	1.6		8.2	1.00	24	0.44	46	2.75	0.0						T	18

Note: T = <0.25%.

Clinoptilolite

Clinoptilolite appears to be a diagenetic mineral here, replacing and (or) filling radiolarian tests, as indicated by SEM and optical microscope investigations (Plates 3 and 2). It occurs only in Core 70 and at the top of Core 71, and its abundance is closely related to that of smectite; its occurrence is restricted to the smectite-rich sediments which have been interpreted as direct echoes of volcanic events. Because clinoptilolite has a higher silica content than smectite, it implies the availability of free silica during diagenesis. This silica was supplied here in large amounts by dissolution of radiolarian tests (highly soluble amorphous biogenic silica).

Although clinoptilolite does not result here from the direct transformation of volcanic material (as it is often believed to happen in marine sediments), this mineral appears to be closely related to volcanic events.

Quartz (Chalcedony)

Quartz is present throughout the studied section; its X-ray crystallinity[2] and the (100)/(101) peak-height ratio show that quartz is not a terrigenous detrital constituent, but authigenic chalcedony. Chalcedony is a well-known constituent of cherts (Heath and Moberly, 1971; Lancelot, 1973); it has been shown to be derived from highly soluble amorphous biogenic silica (mainly radiolarian tests) through diagenetic processes. SEM observations (Plate 4) show that, through fragmentation and dissolution, radiolarian tests released notable amounts of silica and dissolved silica. The biogenic silica was later converted to chalcedony.

Variations in chalcedony abundance and crystallinity do not show any significant trend, except in the upper part of Core 69, where this mineral disappears almost completely within the limestone matrix, being restricted to discrete chert layers.

Opal-CT

The nomenclature used here follows the definition of Jones and Segnit (1971). Opal-CT is present in considerable amounts in the studied section; it may constitute up to 75% of the sediment.

SEM observations show that it occurs either as lepispheres filling dissolution cavities, or as massive, structureless (at the SEM scale) material constituting the matrix of the sediment—or both. Its diagenetic character, already known from previous studies (Keene, 1976), is obvious here, and it is possible to state that *opal-CT crystallized later than clinoptilolite* (Plates 3 and 4).

Opal-CT occurs in Cores 72, 71, and 70, and at the base of Core 69. (It should be kept in mind that the interval between the base of Core 69 and the top of Core 70, as represented in Figure 3, does not necessarily represent reality, because of partial recovery within Core 69; the base of Core 69 may actually be close to the top of Core 70.) Its abundance, although displaying large variations on a decimetric scale, reaches a maximum throughout Core 70 and in the upper part of Core 71; in this silica-rich section, opal-CT constitutes 40% (average) of the sediment. The large variations of abundance are clearly controlled by the lithology of the host sediment. Opal-CT abundance is in remarkable inverse correlation with smectite abundance. This suggests either the impossibility of opal-CT crystallization in impermeable clayey sediments—no mobility of interstitial water, and/or the presence of foreign cations in large amounts—or dilution of the "snow fall" of radiolarian tests by rapid settling of smectite (volcanogenic material).

The absence of a significant relation between smectite and chalcedony (recrystallized radiolarian debris) abundance does not seem to favor the second hypothesis, and we therefore shall tentatively keep the lithological control hypothesis. This hypothesis implies that notable vertical migration, on a decimetric scale, occurred after dissolution of radolarian tests within the sediment and before crystallization of opal-CT. Nevertheless, despite this vertical migration, resulting in the present distribution of opal-CT, it is possible to characterize the silica-rich sequence (Core 70 and Section 1 of Core 71) by an average value of the opal-CT content, about 40%.

The B/A ratio on the diffractograms (height of "tridymite" peak at 20.6° 2θ CuKα versus height of "cristobalite" peak at 21.6° 2θ CuKα) averages 0.45. This ratio was defined and tentatively used as a maturity index for opal-CT was defined and tentatively used as a maturity index for opal-CT from eastern North Atlantic sediments (Mélières, 1978), where the value 0.45 is indicative of a burial depth of about 600 meters. Here the burial depth of the sediments (although much older) is 610 to 630 meters. This very good agreement between these two locations is encouraging for further investigation.

The presence of opal-CT in considerable amounts suggests that large quantities of biogenic amorphous silica were deposited and later dissolved before being converted to opal-CT. This seems clearly established by the intense dissolution observed in the radiolarian tests (Plate 4). This indicates that large numbers of radiolarians developed in sea water during the time of deposition of Core 70 and the upper part of Core 71. We know that frequent volcanic events occurred during this time; therefore it seems likely that silica was released in sea water through volcanic activity and readily metabolized by radiolarians (high productivity of the siliceous plankton). Consequently, the sedimentation rate should have been considerable during this episode.

Calcite

Except for scarce siderite, calcite is the only carbonate present in the studied section. Besides abundance, special attention was paid to accurate measurement of calcite crystallographic parameters. X-ray crystallinity was measured through slow scanning (0.25° 2θ/min) of the (104) peak; the value given in Table 1 and in Figure 3 is the width at half-height of the (104) peak,

[2] The X-ray crystallinity is the difference between the width at half-height of the (101) peak and the instrumental width; the value is given in 1/10° 2θ (CuKα) in Table 1 and Figure 3.

minus the instrumental width; this value is given in 1/100° 2θ CuKα, the precision being on the order of $\pm 0.005°2\theta$; a perfect crystal has a crystallinity of 0. $MgCo_3$ (mole) content was measured by the angular position of both the (104) peak and the (108) (116) doublet; absolute precision is on the order of $\pm 0.2\%$ $MgCO_3$. (It should be kept in mind that the diffractometry method does not imply that magnesium is the only cation responsible for the shift of the (104) calcite peak, metallic cations smaller than calcium theoretically being able to induce the lattice-contraction effect. Therefore the "$MgCO_3$ content" of calcite determined here is rather an "$MgCO_3$ equivalent"; fortunately, there is high probability of magnesium presence.)

These parameters, together with calcite abundance, allow definition of three zones in the studied section:

1) Core 72 and the lower part of Core 71 (from the base up to about Section 2, 50 cm). Here, calcite is the main constituent of the sediment, averaging 50%. A very good crystallinity and a very low magnesium content indicate that this calcite is biogenic (calcareous nannoplankton), and was diagenetically recrystallized. SEM observation (Plate 5) confirms this interpretation.

2) The upper part of Core 71, all of Core 70, and the base of Core 69 are characterized by low to very low calcite contents (in places complete absence), poor calcite crystallinities, and notable $MgCO_3$ content. This, together with SEM observation (Plate 5), indicates that the calcite is biogenic and underwent considerable dissolution, but was not recrystallized (or weakly recrystallized) during diagenesis. Indeed, dilution of the calcite tests "snow fall" by siliceous biogenic remains (now opal-CT and chalcedony) played a role in the lowering of the calcite content of the sediment, but such dilution cannot account for the complete disappearance of calcite. Therefore, dissolution must have occurred, probably before the settling of the particles, because a post-depositional dissolution would not have eliminated the calcium (at least on the episode scale).

The pre-depositional dissolution of calcite is interpreted as having resulted from an increase of carbon dioxide content of sea water, because of the oxidation of large amounts of organic matter released by the siliceous plankton. Similar processes are thought to have occurred within Aptian sediments from the eastern North Atlantic (Mélières, 1979). The absence of calcite recrystallization is attributed to the impossibility of migration interstitial water, because of the impermeability of the matrix (opal-CT and clay minerals). The fact that magnesian calcite was preserved suggests that the depositional depth was not considerable, probably on the order of a few hundreds of meters or less.

3) In Core 69, after a transitional zone within the lower part, the calcite content rises rapidly and reaches very high and constant values (80–90%), except for chert beds and a few small layers of reworked volcanogenic material. Excellent crystallinity and the absence of magnesium indicate that the calcite results from intense recrystallization of calcitic remains, as is seen in SEM observation. Recrystallization is obviously related to the high porosity existing after sedimentation because of the absence of opal-CT, chalcedony, and clay minerals.

Siderite

Siderite occurs sporadically in minor amounts. It appears as perfect rhombohedrons scattered in thin beds within the more-clayey lithologies. X-ray diffraction shows that it contains up to 10% $CaCO_3$, and X-ray microprobe reveals that calcium distribution in the lattice is not homogeneous. Siderite is therefore thought to be diagenetic, iron probably having been supplied by iron-rich smectites.

Pyrite

Pyrite occurs only in Core 70, but in rather constant amounts (a few percent); single peaks exceed 10%. SEM observation shows that this pyrite is framboidal, and therefore formed in diagenesis; it results from the activity of sulfate-reducing bacteria. This suggests that the sedimentary medium, at least below the first centimeters beneath the sea floor, was characterized by reducing conditions. An active bacterial life within the new-born sediment indicates a high influx of organic matter. The abundance peaks of pyrite correlate well with those of organic carbon, and, in the studied silica-rich interval, the occurrence of pyrite matches exactly that of organic carbon (Fig. 3).

Barite

Barium sulfate occurs in very low amounts (<1%), but almost continuously, throughout Core 70, and much more sporadically in Cores 71 and 72. Because of its very low concentrations, barite was not investigated by SEM; therefore, it is difficult to make any positive statement about its origin. Nevertheless, because of its correlation with the silica-rich interval we tentatively suggest that barium could have originated in the organic material,which settled in large amounts. An organic source for barite in deep-sea barites and the association of barite with organic carbon in deep-sea sediments have been reported often (Dean and Schreiber, 1978).

Halite

Halite does not exist in the sediment as a mineral, but results from evaporation of the interstitial water when the samples dried. Nevertheless, the amount of this halite in the samples is reported for two reasons: (1) from an analytical point of view this "halite" takes part in the quantitive analysis balance, and (2) whatever the origin of the interstitial water of the samples (drilling contamination or genuine), the "halite" content gives an indication of the porosity of the sediment; the distribution of "halite" in the studied sequence confirms this assumption.

Amorphous Material

The amorphous material content is estimated by subtracting the total amount of crystallized constituents from 100. This actually yields only rough values, especially in clayey lithologies. Amorphous material is present throughout the studied section; its content averages 20% and displays notable variations. In Cores 71 and 72, these variations appear in good correlation with smectite abundance. Because smectite is directly related to volcanogenic material, it seems that amorphous material proceeds from the same sources and therefore probably consists mainly of terrigenous alumino-silicates. In Cores 70 and 69, the variations do not appear to be related to variations in other constituents; the only notable feature is a slight decrease within the calcareous material in the upper part of Core 69, suggesting that the amorphous material is terrigenous.

Plant debris occurs throughout Core 70. It consists of fragile black (carbonized) microscopic ribbons deposited within the sediment interbeds; the plants which provided this material were gymnosperms (Plate 6). The plant debris implies relative proximity of land masses; this confirms the indications of terrigenous K-feldspar and kaolinite (463-72-2, 13–14 cm).

Phosphate grains occur in Core 70 within the layers richest in organic carbon. They consist of minute brown flakes, probably fish scales (Plate 6). They indicate a depositional environment at times reducing enough to preserve fish remains. This confirms the indications of the mineral assemblage.

ORGANIC MATTER

From 463-72-2, 102 cm to 463-70-1, 4 cm, the sediment contains 40 to 60% by weight carbonate (5–7% mineral carbon), except for the intermediate interval 463-71-1, 123 cm to 463-70-2, 53 cm, where the carbonate content ranges from 0 to 30% (0–4% mineral carbon).

Organic Carbon

The vertical distribution of organic carbon is shown in Figures 3 and 4.

Organic-carbon contents of 0.04 to 0.25% characterizes the two extreme carbonate intervals, whereas higher contents ranging from 0.07 to 7% define the intermediate intervals. A detailed examination of the latter permits recognition of three main divisions (A, B, and C in Fig. 4).

Interval A shows a marked change between 463-70-6, 134 cm and 463-70-6, 123 cm, where subdivision A1, characterized by a low organic-carbon content (<0.25%), passes to the enriched subdivision A2 (0.26–1.00%). The latter is interrupted by two richer layers (≥2%) at 463-70-6, 145 cm to 463-70-6, 35 cm and 463-70-5, 129 cm to 463-70-5, 100 cm.

Interval B has three subdivisions, with progressively increasing organic-carbon contents: B1, beginning at 463-70-4, 78 cm, with a content of 0.40% and less; followed at 463-70-3, 117 cm by B2 (0.29–0.62%); and B3 at 463-70-3, 39 cm (0.51–6.94%).

Interval C has three subdivisions. The boundaries are at 463-70-2, 137 cm and 463-70-2, 91 cm. The increase observed for Interval B exists also in Interval C.

Pyrolysis Assay

METHODOLOGY

A Rock Eval apparatus was used in pyrolysis. Pyrolysis assay (Espitalié et al., 1977a, b) of raw samples was a simulation of the elemental analysis method for kerogen (Tissot et al., 1974). Two parameters, oxygen index (OI) and hydrogen index (HI), allow characterization of the organic matter in the same way that the Van Krevelen diagram (H/C versus O/C) can be used for the kerogen concentrate. Thus, they define the same three types of organic matter, types I, II, and III. Kerogens of type III derive mainly from plant debris and humic continental matter. Kerogens of types I or II represent aquatic organic material, in which the proportions of planktonic, nektonic, and benthic organisms depend on environmental factors.

Moreover, a correlation between the experimental temperature reached at the maximum of hydrocarbon production during pyrolysis (S2 peak temperature) and the maturation stages of the kerogen was established. The 400 to 435°C range corresponds to the immature-kerogen zone, the 435 to 460°C range to the zone of main oil genesis, and beyond 460°C to the gas or cracking zone.

Maturation of Studied Samples (Table 2)

For the interval 463-71-2, 31 cm and 463-69-3, 14 cm (interval of pyrolysis study), the significant temperatures range from 405 to 430°C. This corresponds to the immature zone, where vitrinite reflectances are less than 0.5. At such a low stage of maturation, the observed variations of pyrolysis indexes are probably more dependent on the organic-matter composition than on maturation. Some overmatured materials were also detected at various places in the interval; they correspond to temperatures of 490°C and more and probably represent high-temperature thermal alteration (volcanic effects?).

Yield of Hydrocarbons (Table 2, Fig. 4)

If the yields of hydrocarbons (HC) obtained from pyrolysis of kerogen (= hydrogen index related to weight of rock) are considered (Table 2), the vertical distribution (Fig. 4) is largely comparable to that of organic carbon, according to the three following classes: (1) 0 to 0.20 mg of HC per gram of rock; (2) 0.21 to 1.50 mg/g; and (3) 1.51 to 30.00 mg/g.

The relation between organic carbon and the yield of pyrolysis HC indicates a relative homogeneous composition for the analyzed organic matter. However, despite a fair correlation, some discrepancies are detected. In subdivision A2 for instance, comparable organic carbon contents in 463-70-6, 22 cm and 463-70-5, 47 cm (0.63 and 0.68%) correspond to HC yields of 0.97 and 0.67 mg/g, respectively. Likewise, at 463-70-6, 13 cm and 463-70-5, 1 cm (organic carbon of 0.53 and 0.71%) HC yields are 0.56 and 0.30 mg/gram. Such differences in pyrolysis yield imply some variations in organic-matter composition, and a detailed characterization of organic matter was therefore undertaken.

Characterization of Organic Matter (Fig. 5)

The samples richest in organic carbon (≥3%) reveal the highest hydrogen indexes (≥350) and the lowest

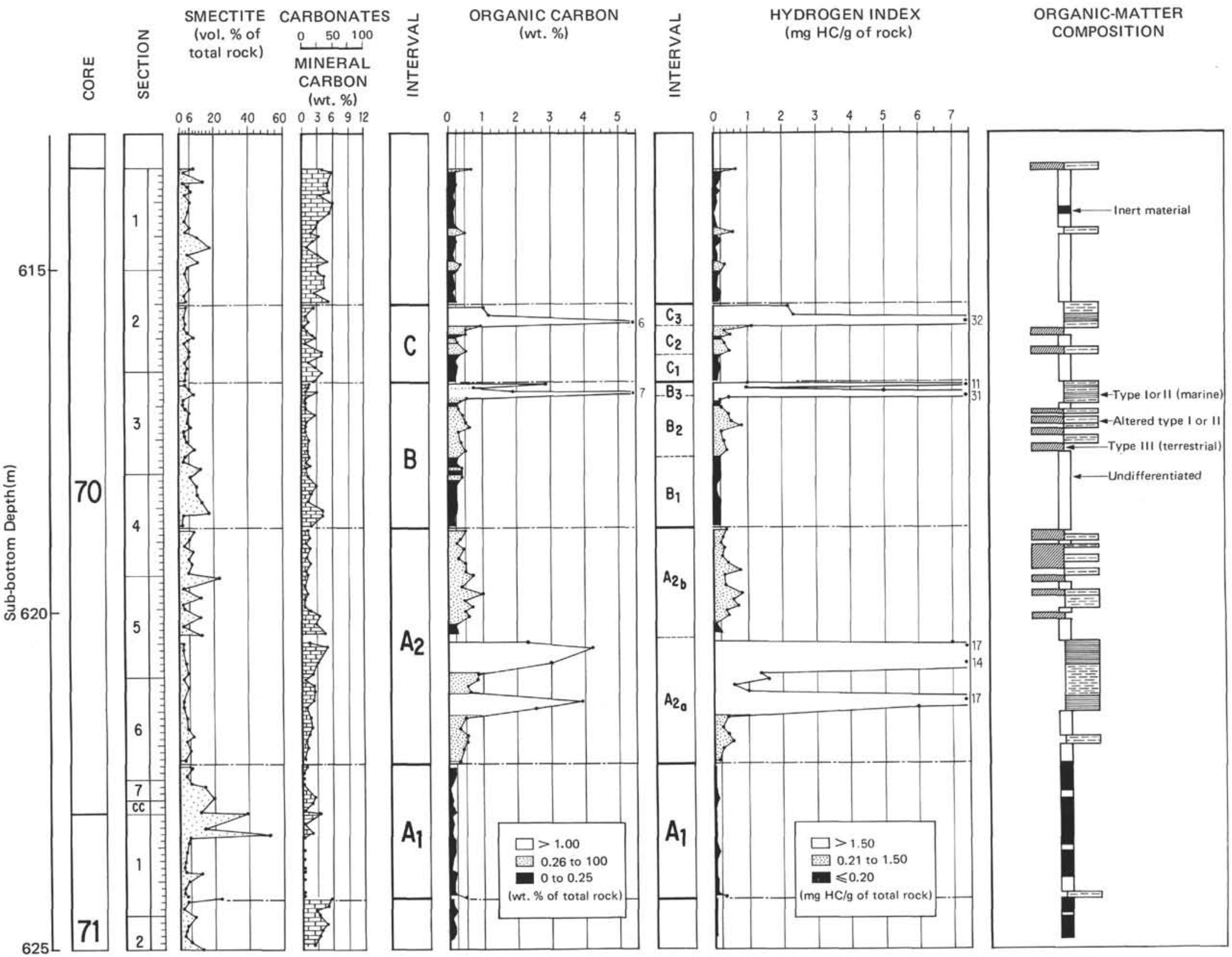

Figure 4. Organic-geochemistry profiles, Cores 70 and 71, Site 463.

Table 2. Geochemical data, Site 463, Cores 69 through 71.

Interval	Sample (interval in cm)	Sub-bottom Depth (m)	Mineral Carbon (wt. %)	Organic Carbon (wt. %)	Hydrogen Index (mg HC/g org. C)	Oxygen Index (mg CO_2/g org. C)	Hydrogen Index (mg HC/g rock)	Oxygen Index (mg CO_2/g rock)	Pyrolysis Temperature (°C)
	463-69-3, 14–15	607.14	6.4	0.16	49	931	0.08	1.49	422
	69-3, 22–24	607.22	5.8	0.20	60	390	0.12	0.78	408
	69-3, 31–32	607.31	4.4	0.13	52	1523	0.07	1.98	422
	69-3, 39–41	607.39	3.2	0.22	97	955	0.21	2.10	420
	69-3, 46–48	607.46	4.5	0.14	102	1429	0.14	2.00	418
	70-1, 4–5	613.54	3.8	0.68	90	218	0.61	1.48	426
	70-1, 7–8	613.57	5.6	0.21	117	1186	0.25	2.49	420
	70-1, 23–24	613.73	4.8	0.23	45	457	0.10	1.05	427
	70-1, 27–29	613.77	4.8	0.33	22	497	0.07	1.64	415
	70-1, 37–38	613.87	5.2	0.17	80	765	0.14	1.30	409
	70-1, 41–43	613.91	3.4	0.15	54	1093	0.08	1.64	415
	70-1, 52–53	614.02	6.0	0.19	47	779	0.09	1.48	422
	70-1, 67–68	614.17	5.3	0.15	0	927	0.00	1.39	
	70-1, 80–82	614.30	3.0	0.16	35	1375	0.06	2.20	425
	70-1, 89–91	614.39	2.6	0.25	35	560	0.09	1.40	373?
	70-1, 96–98	614.46	1.7	0.49	112	359	0.55	1.76	413
	70-1, 101–102	614.51	3.0	0.16	41	1438	0.07	2.30	408
	70-1, 108–109	614.58	2.0	0.30	77	573	0.23	1.72	413
	70-1, 117–118	614.57	0.7	0.23	2	217	0.00	0.50	
	70-1, 128–130	614.78	2.8	0.13	60	1762	0.08	2.29	419
	70-1, 138–139	614.88	4.8	0.18	45	394	0.08	0.71	365?
	70-1, 143–145	614.93	3.2	0.35	93	634	0.32	2.22	419
	70-2, 4–5	615.04	3.2	0.25	72	828	0.18	2.07	424
	70-2, 9–10	615.09	4.2	0.13	96	1569	0.13	2.04	415
	70-2, 27–29	615.27	4.2	0.20	39	440	0.08	0.88	417
	70-2, 34–35	615.34	2.4	0.14	132	1214	0.18	1.70	409
	70-2, 46–47	615.46	5.2	0.20	64	1065	0.13	2.13	417
C3	70-2, 53–54	615.53	2.5	1.03	210	190	2.16	1.96	430
	70-2, 68–70	615.68	0.6	1.18	197	118	2.32	1.39	425+
	70-2, 77–78	615.77	1.0	6.22	521	51	32.43	3.19	417
	70-2, 85–86	615.85	0.1	0.94	120	61	1.13	0.57	411
C2	70-2, 91–94	615.91	0.9	0.49	58	173	0.29	0.85	408
	70-2, 97–99	615.97	1.9	0.50	97	198	0.48	0.99	416
	70-2, 101–103	616.01	2.3	0.20	95	890	0.19	1.78	410
	70-2, 109–111	616.09	0.5	0.26	119	408	0.31	1.06	423
	70-2, 121–122	616.21	3.7	0.53	85	208	0.45	1.10	413
	70-2, 127–129	616.27	3.7	0.32	59	328	0.19	1.05	418
C1	70-2, 137–139	616.37	1.2	0.22	63	682	0.14	1.50	421
	70-2, 144–146	616.44	2.4	0.30	68	443	0.20	1.33	418
	70-3, 2–3	616.52	3.7	0.25	60	1060	0.15	2.65	403
	70-3, 16–17	616.66	2.2	0.18	57	822	0.10	1.49	415
B3	70-3, 19–20	616.69	1.1	0.59	165	278	0.97	1.64	422+
	70-3, 20–21	616.70	1.6	2.87	393	89	11.27	2.55	424
	70-3, 25–27	616.75	0.9	0.73	131	162	0.95	1.18	414
	70-3, 30–31	616.80	0.5	1.90	265	105	5.04	1.99	430
	70-3, 31–32	616.81	2.8	6.94	451	61	31.29	4.24	419
	70-3, 39–40	616.89	0.5	0.51	83	100	0.42	0.51	409
B2	70-3, 43–44	616.93	0.2	0.34	49	229	0.17	0.78	418
	70-3, 47–49	616.97	0.4	0.27	51	130	0.14	0.35	410+
	70-3, 55–56	617.05	0.8	0.28	76	268	0.21	0.75	433+
	70-3, 64–65	617.14	2.2	0.41	107	437	0.44	1.79	418
	70-3, 75–77	617.25	0.9	0.52	98	167	0.51	0.87	421
	70-3, 81–82	617.31	0.7	0.62	132	102	0.82	0.63	404
	70-3, 89–90	617.39	0.7	0.29	76	197	0.22	0.57	418
	70-3, 103–104	617.53	1.4	0.38	81	308	0.31	1.17	403
	70-3, 117–119	617.67	1.1	0.47	79	196	0.37	0.92	422
B1	70-3, 127–129	617.77	1.3	0.28	59	446	0.16	1.25	415
	70-3, 134–136	617.84	0.9	0.24	59	488	0.14	1.17	408+
	70-3, 140–142	617.90	1.4	0.26	85	496	0.24	1.39	431
	70-3, 142–144	617.92	0.8	0.37	37	351	0.14	1.30	410
	70-4, 5–7	618.05	1.2	0.40	60	280	0.24	1.12	421
	70-4, 18–20	618.18	2.9	0.28	27	211	0.07	0.59	416
	70-4, 31–32	618.31	1.7	0.24	41	413	0.10	0.99	395?
	70-4, 42–43	618.42	1.2	0.25	73	320	0.18	0.80	368?
	70-4, 56–57	618.56	3.9	0.26	50	242	0.13	0.63	427
	70-4, 63–64	618.63	3.9	0.18	80	889	0.14	1.60	405+
	70-4, 78–79	618.78	1.6	0.20	86	750	0.17	1.50	419
$A2_b$	70-4, 84–85	618.84	1.0	0.48	74	133	0.36	0.54	413
	70-4, 96–97	618.96	1.3	0.34	71	253	0.24	0.86	424
	70-4, 104–105	619.04	0.6	0.24	78	283	0.19	0.68	418
	70-4, 111–113	619.11	1.5	0.44	67	225	0.30	0.99	422
	70-4, 124–125	619.24	0.8	0.31	80	258	0.25	0.80	410
	70-4, 133–135	619.33	1.5	0.48	85	194	0.41	0.93	427+
	70-4, 144–145	619.44	0.8	0.50	151	64	0.76	0.32	416
	70-5, 0–1	619.50	1.0	0.71	43	132	0.30	0.94	410
	70-5, 16–17	619.66	0.4	0.40	80	703	0.32	2.81	417
	70-5, 27–28	619.77	1.0	1.00	80	124	0.80	1.24	406
	70-5, 37–38	619.87	0.3	0.44	122	184	0.54	0.81	419
	70-5, 47–48	619.97	0.4	0.68	99	213	0.67	1.45	415
	70-5, 53–54	620.03	1.3	0.47	73	368	0.34	1.73	410
	70-5, 60–61	620.10	3.1	0.58	66	167	0.38	0.97	413
	70-5, 72–73	620.22	2.7	0.23	20	900	0.05	2.07	
	70-5, 84–85	620.34	4.1	0.38	48	266	0.18	1.01	410
$A2_a$	70-5, 100–101	620.50	1.2	2.32	294	93	6.82	2.15	411
	70-5, 106–108	620.56	4.6	4.24	408	101	17.31	4.30	413
	70-5, 129–130	620.79	2.8	3.00	469	103	14.07	3.10	416
	70-5, 146–147	620.96	1.8	0.86	158	213	1.36	1.93	419
	70-6, 4–5	621.04	0.4	0.82	192	196	1.58	1.61	423
	70-6, 13–14	621.13	2.0	0.53	105	319	0.56	1.69	416
	70-6, 23–24	621.23	2.2	0.63	155	249	0.97	1.57	422
	70-6, 35–36	621.35	2.0	3.92	431	80	16.91	3.13	415
	70-6, 45–46	621.45	0.8	2.55	243	88	6.21	2.24	418

Table 2. (Continued).

Interval	Sample (interval in cm)	Sub-bottom Depth (m)	Mineral Carbon (wt. %)	Organic Carbon (wt. %)	Hydrogen Index (mg HC/ g org. C)	Oxygen Index (mg CO_2/ g org. C)	Hydrogen Index (mg HC/ g rock)	Oxygen Index (mg CO_2/ g rock)	Pyrolysis Temperature (°C)
$A2_a$	70-6, 60-61	621.60	1.4	0.50	74	462	0.37	2.31	408
	70-6, 75-76	621.75	1.6	0.33	63	648	0.21	2.14	411
	70-6, 85-86	621.85	1.2	0.54	68	391	0.37	2.11	413
	70-6, 95-96	621.95	0.5	0.52	99	298	0.51	1.55	416
	70-6, 105-106	622.05	1.1	0.40	55	380	0.22	1.52	416
	70-6, 122-123	622.22	0.3	0.31	37	448	0.11	1.39	415
A1	70-6, 134-135	622.34	0.7	0.16	0	406	0.00	0.55	
	70-6, 144-145	622.44	0.2	0.17	0	400	0.00	0.68	
	70-7, 2-3	622.52	0.2	0.11	0	455	0.00	0.50	
	70-7, 10-11	622.60	0.3	0.06	0	417	0.00	0.25	
	70-7, 29-30	622.70	2.3	0.09	85	878	0.08	0.79	
	70,CC, 8-9	622.88	1.7	0.08	0	887	0.00	0.71	
	70,CC, 18-19	622.98	0.3	0.13	0	254	0.00	0.88	
	71-1, 2-3	623.02	3.4	0.07	0	1857	0.00	1.80	
	71-1, 17-19	623.17	0.3	0.09	0	156	0.00	0.14	
	71-1, 32-33	623.32	1.6	0.09	0	656	0.00	0.59	
	71-1, 38-39	623.38	0.3	0.14	0	386	0.00	0.54	
	71-1, 56-58	623.56	0.3	0.17	60	400	0.10	0.68	391?
	71-1, 69-71	623.69	0.1	0.09	0	44	0.00	0.04	
	71-1, 83-84	623.83	0.4	0.07	0	686	0.00	0.48	
	71-1, 87-89	623.87	0.3	0.16	0	294	0.00	0.47	
	71-1, 98-99	623.98	0.1	0.12	43	200	0.05	0.24	
	71-1, 117-118	624.17	0.1	0.13	17	169	0.02	0.22	
	71-1, 123-124	624.23	0.2	0.45	64	102	0.29	0.46	421 +
	71-1, 127-128	624.27	5.4	0.08	0	1313	0.00	1.05	
	71-1, 138-139	624.38	4.8	0.12	0	1742	0.00	2.09	
	71-1, 144-145	624.44	2.6	0.19	20	732	0.04	1.39	533
	71-2, 2-3	624.52	3.0	0.08	0	2688	0.00	2.15	
	71-2, 14-15	624.64	4.7	0.14	0	386	0.00	0.54	
	71-2, 23-25	624.73	3.6	0.16	0	1281	0.00	2.05	
	71-2, 31-32	624.81	3.2	0.09	0	2289	0.00	2.06	

Note: + = addition peak ≥550°C.

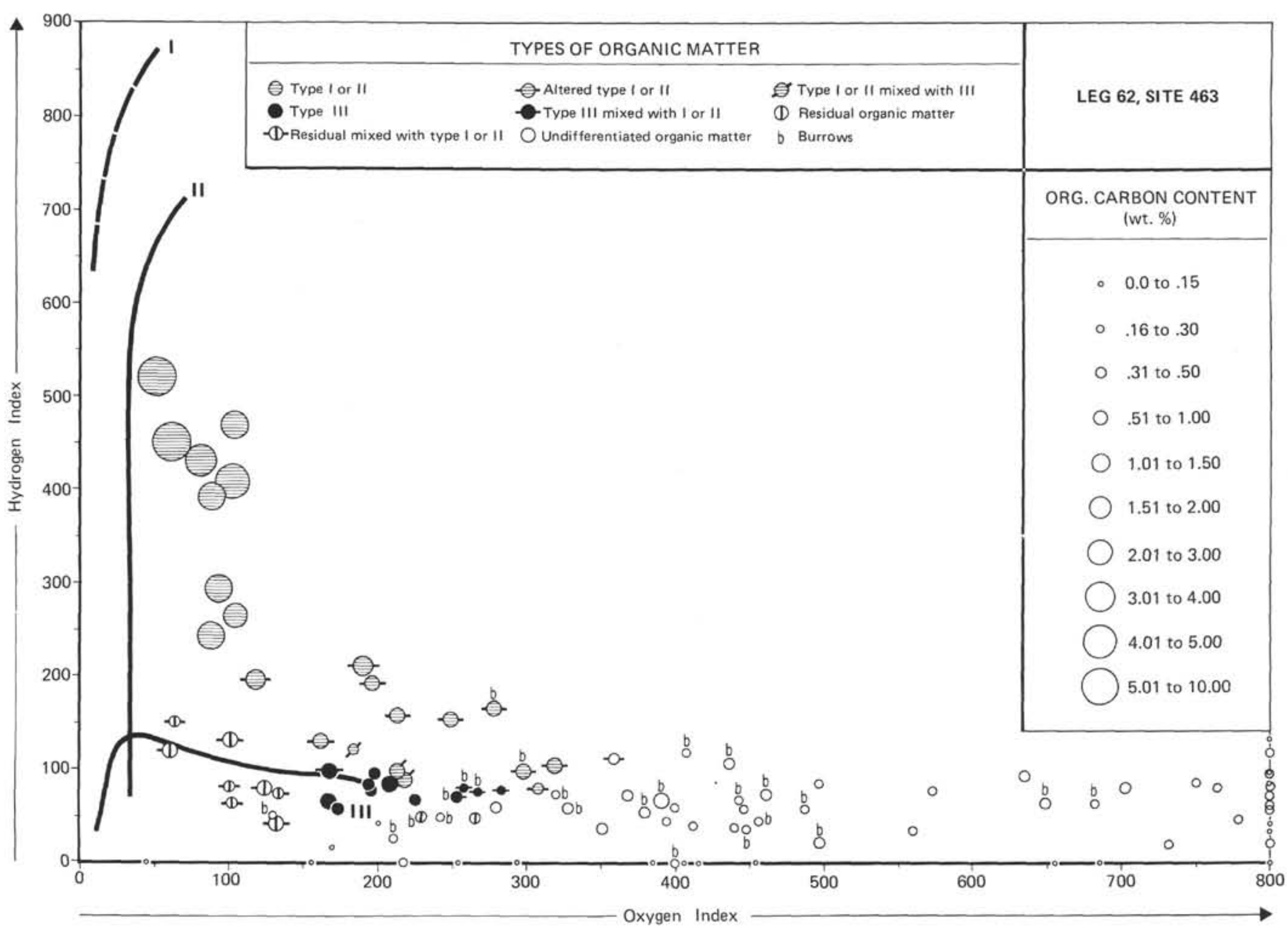

Figure 5. Pyrolysis assays, (hydrogen and oxygen indexes; data related to organic carbon).

oxygen indexes (≤ 100). They contain predominantly aquatic material of type I or II, and paleontological evidence from shipboard studies (Site 463 report, this volume) indicates a marine origin for this aquatic material. An oxygen-poor depositional environment is required to preserve such material and to account for the lamination of the deposits.

Marine organic matter also characterizes samples having 1.9 to 2.5% organic carbon, but the lower HI (200–300) can be explained by dilution of the pyrolyzable material either by inert carbon or by low-hydrogen compounds. More-open environments must have alternated with reducing ones during this sedimentation.

Samples with 1.20 to 0.50% organic carbon have somewhat lower hydrogen indexes, but the variations of OI identify a population with low OI (60–150) and one with high OI (150–400). They both derive from marine material; however, inert and detrital organic matter dilutes the first, whereas the second should be enriched with oxygenated compounds.

In the vicinity of the evolution path of type III (HI 100; OI 150–200), a mixed composition of marine type I or II and of continental humic type III is assumed. Then in the proper area for immature material derived from humic and plant debris of type III (HI $\leq$ 100; OI 200–350) a predominance of detrital and inert organic matter accounts for the lowest HI (<50).

Samples with less than 0.50% organic carbon generally show large oxygen indexes (up to 300) and low hydrogen indexes. Data are too far off reference paths to be significant, and the related organic matter cannot be identified. Hereafter, it is called "undifferentiated."

Samples with the lowest organic-carbon contents ($<0.25\%$) show a nil hydrogen index, while the oxygen indexes are widely variable. Organic matter of these samples is considered to be residual material (Tissot et al., 1979).

Marine organic matter of type I or II is autochthonous, and continental organic matter of type III (inert and residual) is allochthonous. The latter derives either from reworked sedimentary material or from eruptive rocks. Undifferentiated material supposes bad preservation, which can occur both in autochthonous marine and allochthonous continental environments.

Vertical Distribution of Organic-Matter (Fig. 4)

The first marine organic matter appears at 463-71-1, 123 cm, just above a carbonate interval at 463-71-1, 127 cm, where the organic carbon is derived mainly from inert organic matter (Fig. 4). The inert material persists to 463-70-6, 134 cm and characterizes subdivision A1.

At 463-70-6, 123 cm, organic-carbon content increases, but smectite decreases, and pyrite is present instead of siderite. Undifferentiated organic matter is present instead of inert matter from 463-70-6, 123 cm to 463-70-6, 60 cm. Marine organic material reappears at 463-70-6, 95 cm, then characterizes the top of interval $A2_a$ from 463-70-6, 45 cm to 463-70-5, 100 cm.

An abrupt decrease in organic-carbon content is observed at the base of the overlying interval ($A2_b$). The levels richest in organic carbon correspond to the largest amounts of smectite; organic matter derives mainly from continental material (type III) mixed with inert matter. These levels alternate with either undifferentiated or marine organic materials. In turn, the upper part of $A2_b$, from 463-70-5, 1 cm to 463-70-4, 84 cm is characterized by continental organic matter alternating either with mixed marine and terrestrial or undifferentiated organic matter.

Interval B, from 463-70-4, 78 cm to 70-3, 19 cm, comprises a basal zone (B1) of undifferentiated organic matter, as at the bottom of $A2_a$ and $A2_b$. Then, an alternation of marine and continental material defines B2 from 463-70-3, 117 cm to 463-70-3, 43 cm, as for $A2_b$. Interval B3, with typical marine material, follows, and is like the upper part of $A2_a$. In Interval B, the highest content of smectite (up to 6%) is found at the base of subdivision B1.

Three zones are also present in Interval C (i.e., 463-70-3, 16 cm to 463-70-2, 53 cm). They include a zone of undifferentiated organic matter (C1), a zone of mixed organic matter (C2) above 463-70-2, 137 cm, and a zone of marine organic matter (C3) above 463-70-2, 91 cm.

Thereafter, the major change of carbonate content observed from 463-70-2, 46 cm corresponds to an abrupt impoverishment in organic carbon. The corresponding organic matter is undifferentiated material, except for two rich levels at 463-70-1, 96 cm and 463-70-1, 4 cm, where more or less altered marine material is present.

Organic Matter and Sedimentation

Sediments of the 11.3-meter studied interval contain three horizons of high organic-matter content which correspond to a well-preserved marine organic matter and imply an oxygen-poor depositional environment. Also, influxes of inert organic matter (volcanic origin?) as well as terrestrial matter are defined. Terrestrial matter is commonly mixed with more or less altered marine organic matter.

The vertical distribution shows rhythmic sedimentation of organic matter, and several sequences can be defined. Each sequence comprises, from the base to the top, (1) a lower member, where undifferentiated organic matter is associated with light-colored sediments; burrowing is common and pyrite poorly represented in these sediments; (2) a middle member, where terrestrial and more or less altered marine materials are mixed or alternate; and (3) an upper member, of wholly marine organic matter, showing dark, fine parallel laminations.

The analyzed sequence begins with subdivision Al, where inert organic matter is predominant, and the notable smectite content indicates influx of non-marine matter. An incomplete sequence with the middle member missing corresponds to $A2_a$, whereas the upper marine member is absent in the next sequence, $A2_b$. The two last intervals, B and C, correspond to complete sequences with respective thicknesses of 2.08 and 1.13 meters. An abrupt change is then observed at top of C:

the carbonate content increases, and an abrupt decrease in organic matter content indicates the reappearance of undifferentiated organic matter.

CONCLUSIONS

A 15-meter sequence of silica-rich sediments was deposited during the early Aptian in the western Mid-Pacific Mountains (Site 463). The main feature of the mineral assemblage is the fact that the most important part of the sediment now consists of diagenetic species. The sedimentary record of depositional conditions is therefore obscured. Nevertheless, it is possible to sketch the history of the episode as follows.

In the vicinity of emergent land masses, a considerable amount of silica from altered volcanic material was released into sea water through sustained volcanic activity. This silica was readily metabolized by the siliceous plankton, the productivity of which increased markedly. Consequently, (1) large amounts of amorphous silica (radiolarian tests) settled; this material was later diagenetically transformed into opal-CT, chalcedony, and clinoptilolite; (2) large amounts of carbon dioxide were generated in the sea-water column through oxidization of the organic matter, resulting in dissolution of calcareous planktonic tests before they settled; (3) a notable amount of organic matter was able to reach the bottom of the sea and was incorporated within the sediment because of the oxygen-poor depositional environment and high sedimentation rate.

When the volcanic activity ceased, normal calcareous marine sedimentation restarted, yielding oozes, later diagenetically transformed into limestones.

Except for some reworked material, an immature step of evolution is assigned to the studied organic matter. The organic matter originated in two sources: an autochthonous source for the marine material, and an allochthonous source for the humic material and plant debris. The latter probably originated from an adjacent land area. Some residual organic matter was also detected; it could have been derived from terrestrial material influenced by volcanic activity.

An oxygen-poor depositional environment was required to preserve the organic matter of marine origin and to account for the several organic-rich and laminated layers.

Rhythmic sedimentation characterizes the distribution of the organic matter in the studied silica-rich interval. This is based on two adjacent sequences in the upper 3.30 meters of the interval. Each sequence shows an upward progressive increase in organic-carbon content; it begins with a member of undifferentiated organic matter, followed by a member of mixed marine and terrestrial materials, then by a member of abundant, entirely marine organic matter. The underlying 3.50 meters are attributed to two incomplete sequences. The basal 2 meters of the interval contains predominantly inert organic material, as found in the underlying carbonate-rich and organic-matter-poor interval.

ACKNOWLEDGMENTS

The authors thank J. Thiede and T. Vallier, Leg 62 Co-Chief Scientists, for entrusting them with this study. The mineralogical studies received financial support from CNEXO (grant 78/1951), and F. Mélières warmly acknowledges Mr. Lenoble for his cooperation. DTA analyses were carried out at Université d'Orsay (France) under supervision of Dr. A. Desprairies. The manuscript benefited from the reviews of Pr. R. Létolle (Université Pierre et Marie Curie, Paris) and Dr. L. Montadert (Institut Français du Pétrole).

REFERENCES

Dean, W. E., and Schreiber, B. C., 1978. Authigenic barite, Leg 41 Deep Sea Drilling Project. *In* Lancelot, Y., Seibold, E., et al., *Init. Repts. DSDP*, 41: Washington (U.S. Govt. Printing Office), 915–931.

Espitalié, J., Laporte, J. L., Madec, M., et al., 1977. Méthode rapide de caractérisation des roches mères, de leur potentiel pétrolier et de leur degré d'évolution. *Rev. Inst. Franç. Pétrole*, 32:23–42.

Espitalié, J., Madec, M., Tissot, B., et al., 1977. Source rock characterization method for petroleum exploration. Offshore Technology Conference, Houston, Texas, Paper 2935, pp. 439–444.

Heath, G. R., and Moberly, R., 1971. Cherts from the western Pacific, Leg 7, Deep Sea Drilling Project. *In* Winterer, E. L., Riedel, W. R., et al., *Init. Repts. DSDP*, 7, Pt. 2: Washington (U.S. Govt. Printing Office), 991–1007.

Jones, J. B., and Segnit, E. R., 1971. The nature of opal. I. Nomenclature and constituents phases. *J. Geol. Soc. Australia*, 18:57–68.

Keene, J. B., 1976. The distribution, mineralogy and petrography of biogenic and authigenic silica from the Pacific Basin [Ph.D. dissert.]. University of California, San Diego.

Lancelot, Y., 1973. Chert and silica diagenesis in sediments from the central Pacific. *In* Winterer, E. L., Ewing, J. I., et al., *Init. Repts. DSDP*, 17: Washington (U.S. Govt. Printing Office), 377–405.

Mélières, F., 1974. Recherches sur la dynamique sédimentaire du Golfe de Cadix (Espagne) [Thèse]. Université Pierre et Marie Curie, Paris.

_______, 1978. X-ray mineralogy studies, Leg 41 Deep Sea Drilling Project, Eastern North Atlantic Ocean. *In* Lancelot, Y., Seibold, E., et al., *Init. Repts. DSDP*, 41: Washington (U.S. Govt. Printing Office), 1065–1086.

_______, 1979. Mineralogy and geochemistry of selected Albian sediments from the Bay of Biscay, Deep Sea Drilling Project Leg 48. *In* Montadert, L., Roberts, D. G., et al., *Init. Repts. DSDP*, 48: Washington (U.S. Govt. Printing Office), 855–875.

Mélières, F., and Person, A., 1978. Genèse de smectites ferrifères par altération deutérique de la base de coulées volcaniques du Massif Central Français. *Rev. Geogr. Phys. Geol. Dyn.*, 20:389–398.

Tissot, B., Deroo, G., and Herbin, J. P., 1979. Organic matter in Cretaceous sediments of the North Atlantic: contribution to sedimentology and paleogeography. *In* Talwani, M., Hay, W., and Ryan, W. B. F., (Eds.), *Deep Drilling Results in the Atlantic Ocean: Continental Margins and Paleoenvironment:* Washington (Am. Geophys. Union), pp. 362–374.

Tissot, B., Durand, B., Espitalié, J., et al., 1974. Influence of the nature and diagenesis of organic matter in formation of petroleum. *Bull. Am. Assoc. Petrol. Geol.*, 58: 499–506.

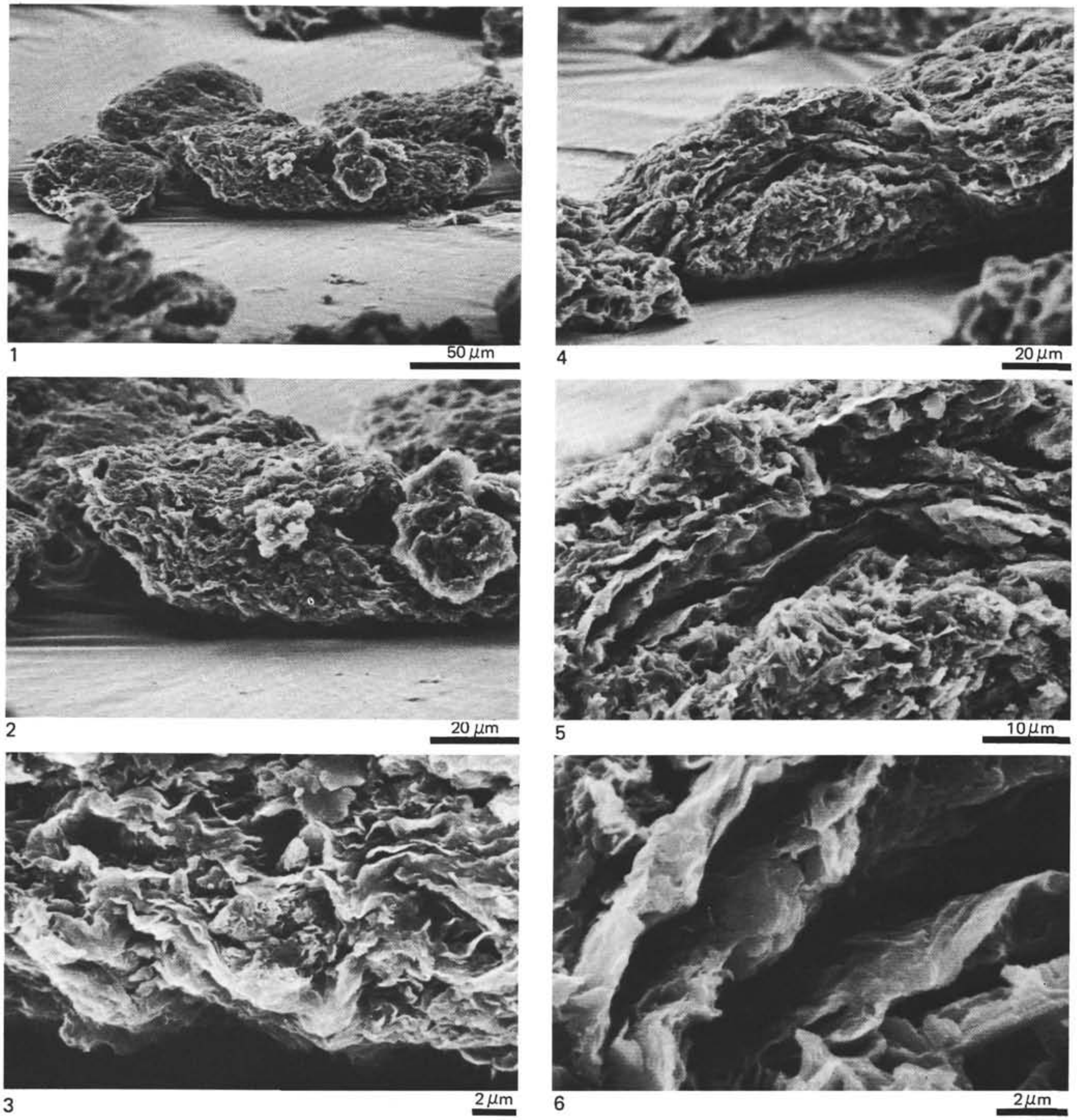

Plate 1. Photomicrographs.

Figure 1-3. Successive SEM close-ups of a volcanic clast completely transformed to smectite. XRD and DTA evidence an iron-bearing beidellite, the structure of which is visible in Figure 3 (flexuous lamellae). This clast is not an aggregate of sedimented clay particles, but a fragment of altered volcanic material. Sample 463-71-1, 32-33 cm.

Figures 4-6. Successive SEM close-ups of a smectitized volcanic clast. The original fluidal structure of the lava fragment is clearly visible. XRD and DTA data as for Figures 1-3. Such clasts, accompanied by clinoptilolitized radiolarians, constitute the main part of the sediment. See also Plate 2. Sample 463-71-1, 32-33 cm.

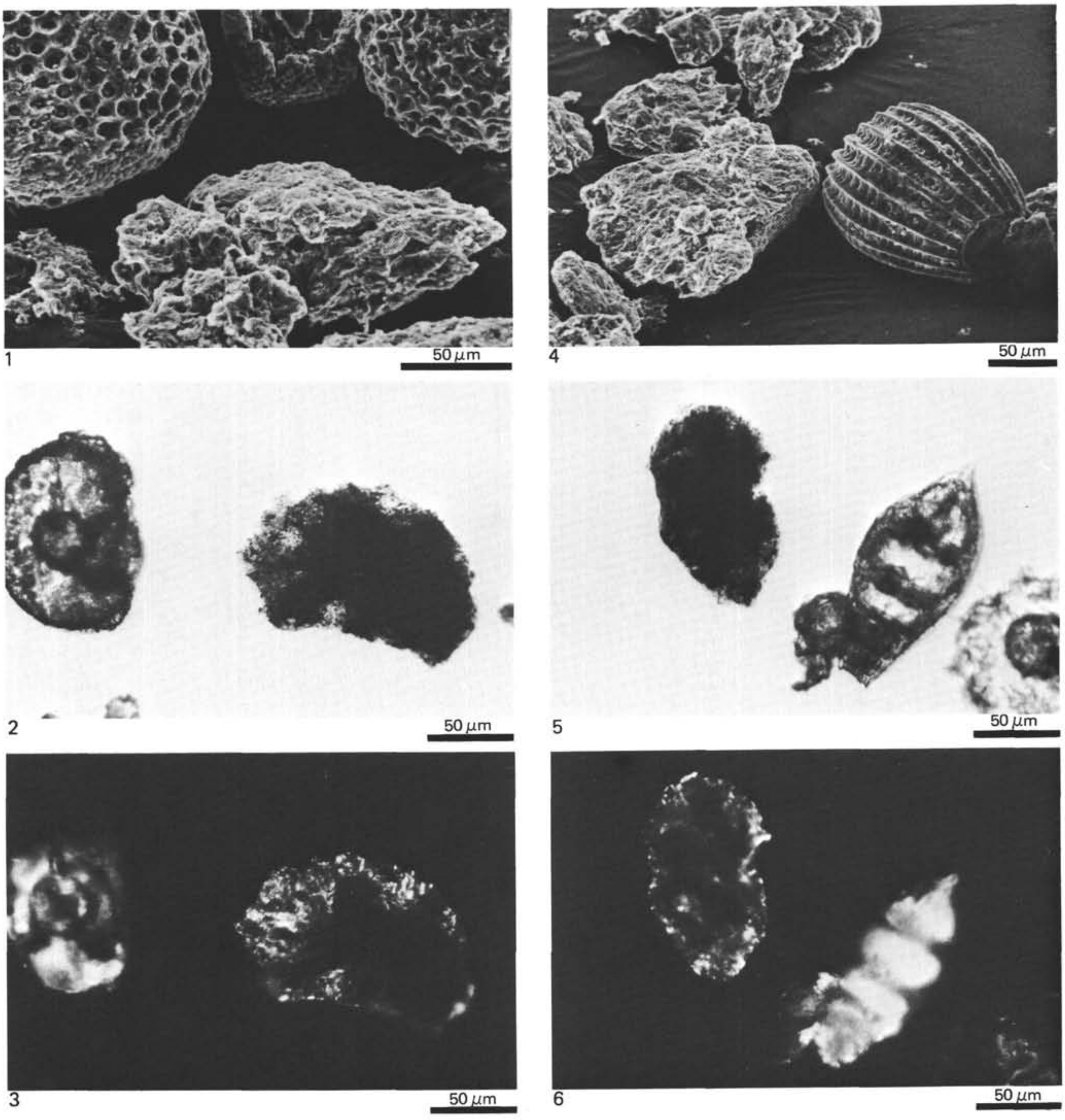

Plate 2. Photomicrographs.

Figures 1–3. SEM (Fig. 1) and optical microscope (Fig. 2, polarized light; Fig. 3, crossed nicols) views of smectite-replaced volcanic clasts. Figure 2 suggests a high iron content, and Figure 3 reveals the crystallized nature (smectite) of the clast. Note the clinoptilolitized radiolarians in the sediment. Sample 463-71-1, 32–33 cm.

Figures 4–6. Example similar to that in Figures 1–3. Note the crystalline nature (crossed nicols) of the volcaniclast. Sample 463-71-1, 32–33 cm.

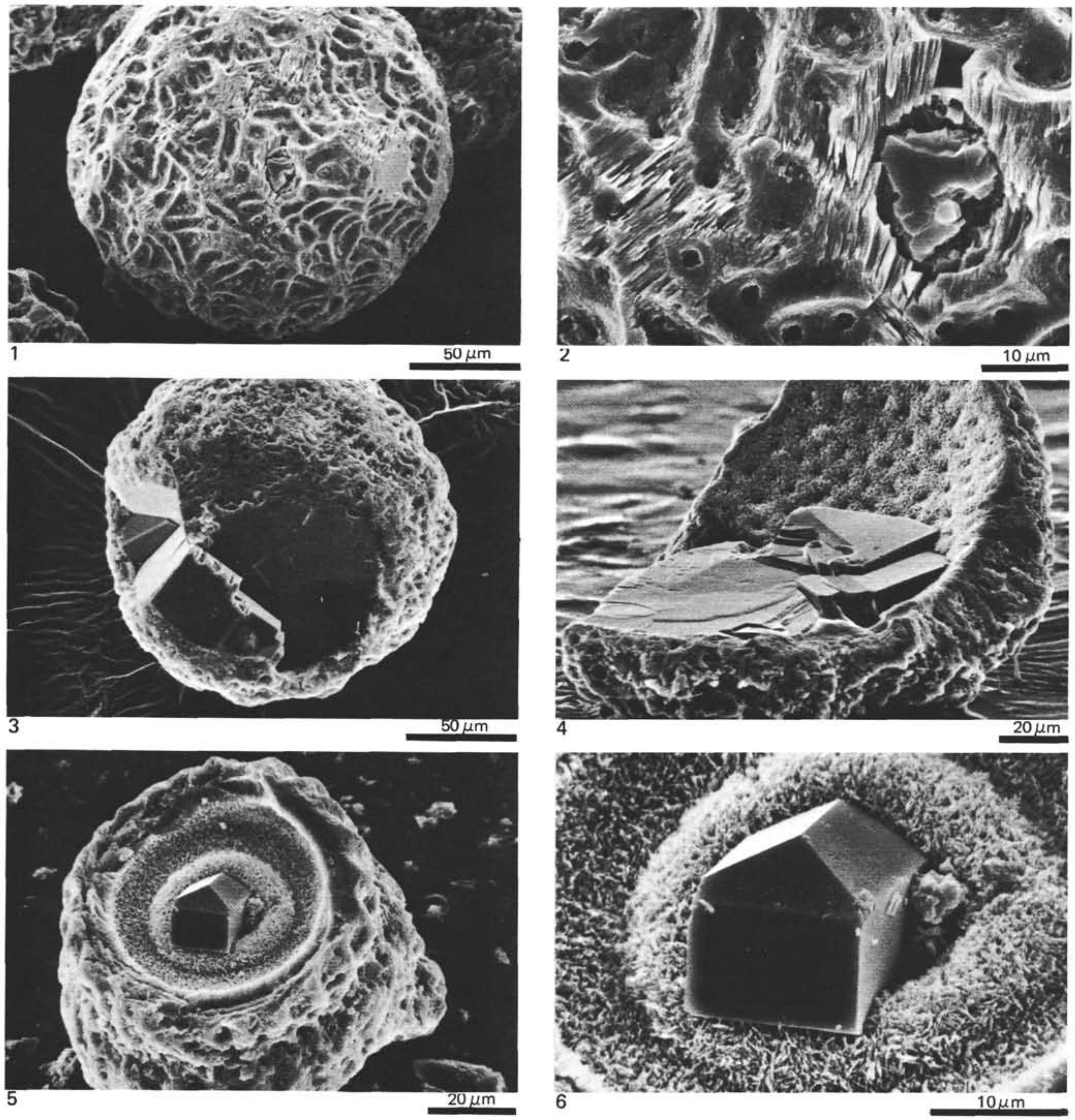

Plate 3. Photomicrographs.

Figure 1. Radiolarian test transformed into clinoptilolite Sample 463-71-1, 32–33 cm.

Figure 2. Close-up of Figure 1 (central part), showing the crystalline nature of the radiolarian test.

Figure 3. Radiolarian replaced by and filled with large, euhedral clinoptilolite crystals. Sample 463-70-4, 18–20 cm.

Figure 4. Clinoptilolite crystals partly filling a fragment of radiolarian test. Note the coating of opal-CT on the inner wall of the test. Sample 463-70-4, 18–20 cm.

Figure 5. Single clinoptilolite crystal within a broken radiolarian test. Sample 463-70-4, 18–20 cm.

Figure 6. Close-up of Figure 5, showing the perfect shape of the clinoptilolite crystal and the coating of opal-CT developed after the growth of clinoptilolite. Sample 463-70-4, 18–20 cm.

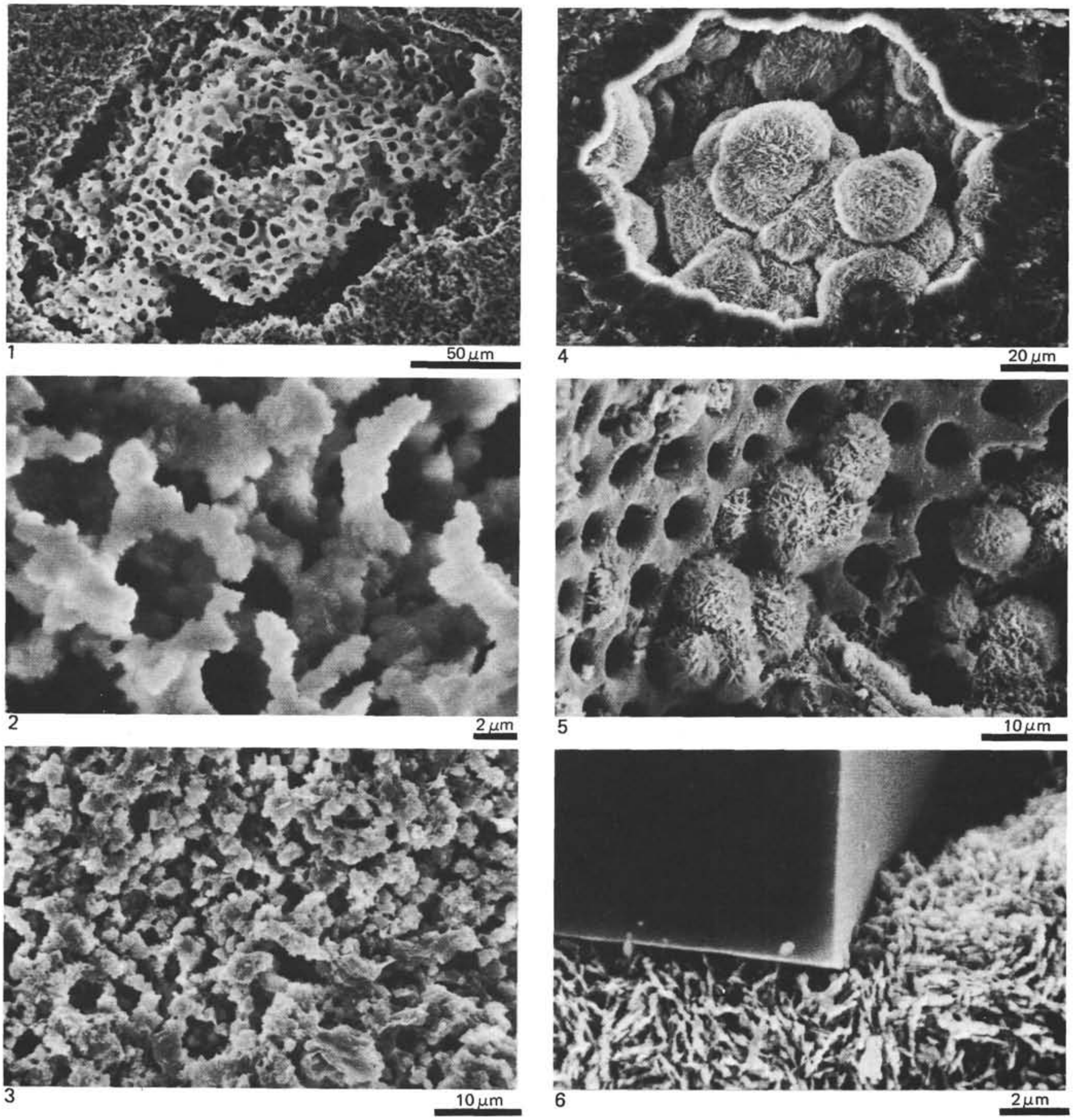

Plate 4. Photomicrographs.

Figure 1. Intensely corroded radiolarian test, now consisting of chalcedony. Sample 463-71-2, 142–144 cm.

Figure 2. Close-up of Figure 1, showing the most intensely corroded part of the radiolarian framework. The corrosion causes the siliceous fragments to collapse, forming the matrix of the sediment. Sample 463-71-2, 142–144 cm.

Figure 3. Matrix of chalcedonic sediment consisting exclusively (XRD) of fragments of intensely corroded radiolarian tests. Sample 463-71-2, 142–144 cm. HCl etched.

Figure 4. Lepispheres of opal-CT in a dissolution cavity. Massive opal-CT constitutes the matrix of the sediment. Sample 463-70-5, 37–38 cm.

Figure 5. Lepispheres of opal-CT in a radiolarian test. Sample 463-70-2, 91–92 cm.

Figure 6. Single crystal of clinoptilolite and blades of opal-CT. Sample 463-70-4, 18–20 cm.

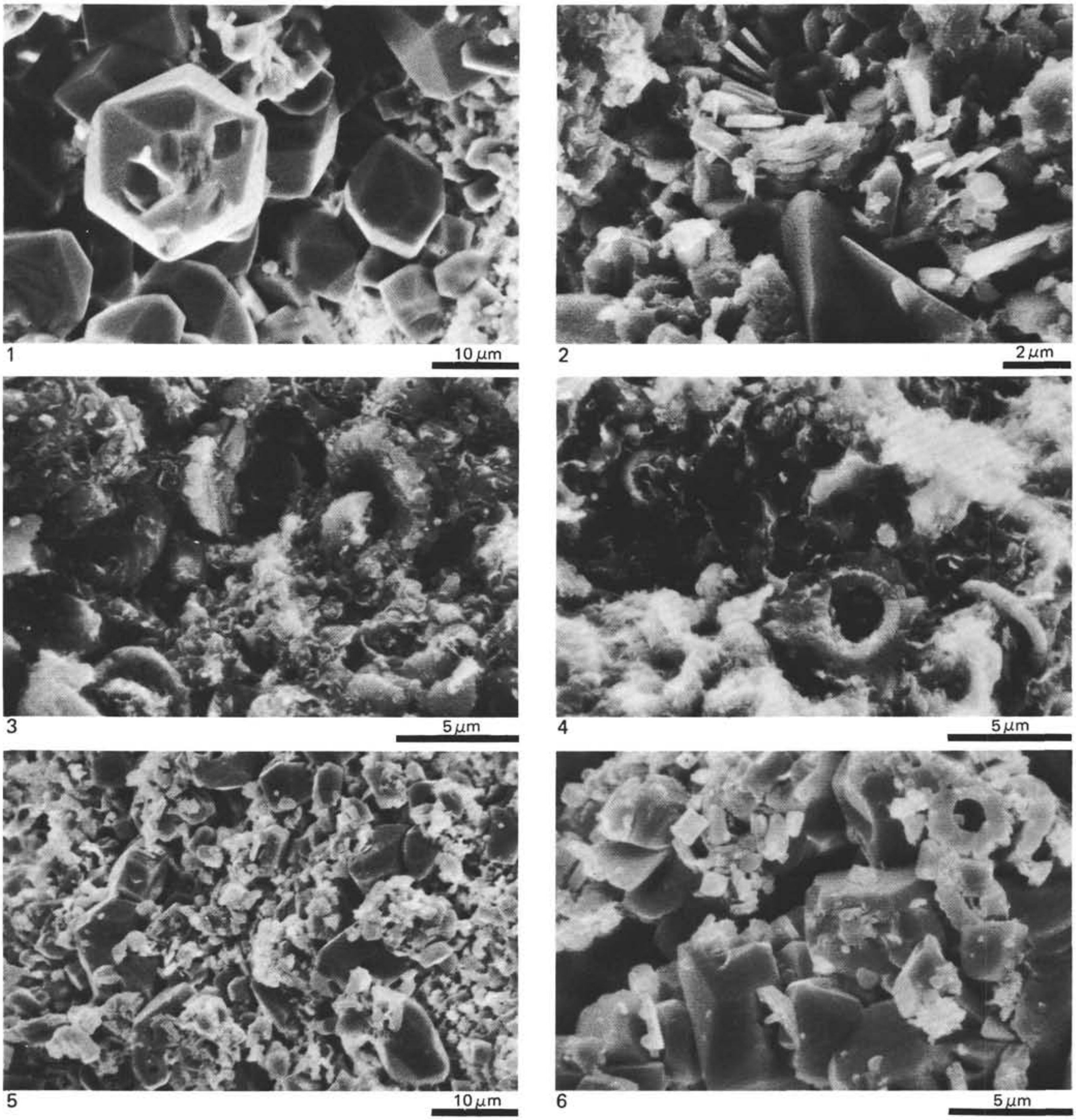

Plate 5. Photomicrographs.

Figures 1, 2. Diagenetic euhedral calcite crystals and recrystallized calcitic biogenic remains. Sample 463-69-1, 140–142 cm.

Figures 3, 4. Non-recrystallized coccoliths (XRD data) in a clayey matrix. Sample 463-70-5, 84–85 cm.

Figures 5, 6. Recrystallized limestone, note the abundant euhedral calcite crystals and rare biogenic remains. Sample 463-71-4, 76–77 cm.

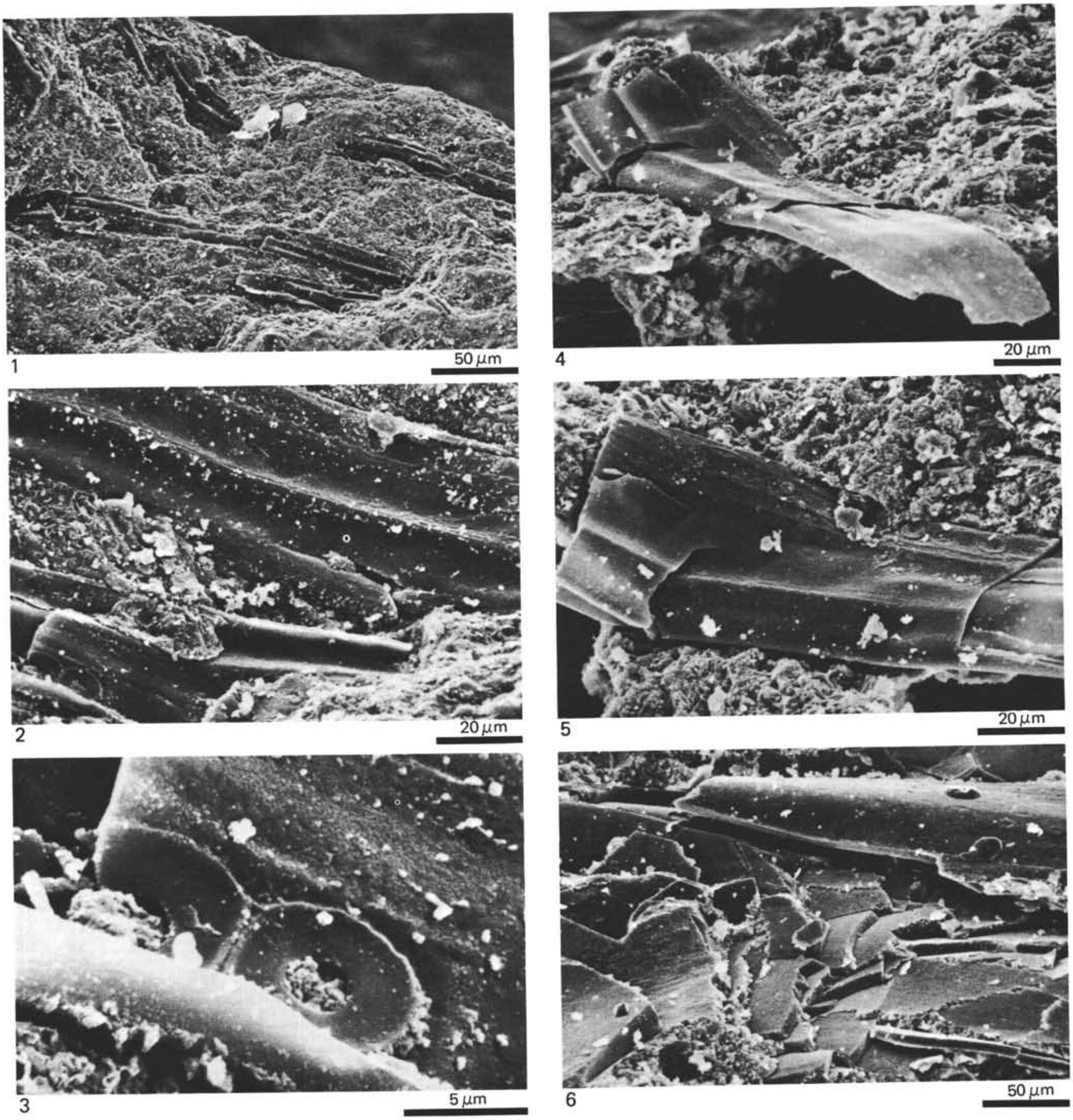

Plate 6. Photomicrographs.

Figure 1–3. Successive SEM close-ups of carbonized plant debris. Radial puncticulations on tracheids identify a gymnosperm fragment. Sample 463-70-3, 19–21 cm.

Figures 4, 5. Two different views of a plant fragment. Note the puncticulations on the upper edge; note also the flattening through compaction. Sample 463-70-5, 105–108 cm.

Figure 6. Organic phosphatic remain (P and Ca from X-ray microprobe data), crushed through compaction. The lamellar structure indicates a fragment of a fish scale.